Half a century of glacier mass balance at Cordilleras Blanca and Huaytapallana, Peruvian Andes

David J. Clark*[1] & Nicholas E. Barrand[1]

[1] School of Geography, Earth & Environmental Sciences, University of Birmingham, UK.

* Corresponding Author: DJC548@alumni.bham.ac.uk

Abstract

The glaciers of the tropical Andes have been observed to be losing mass for much of the last century. These changes are both driven by, and an indicator of global climate change. These glaciers are important as they represent a crucial water source for downstream communities, supplying agriculture, urban usage, industry, mining and hydropower. This study aims to quantify glacial mass loss for the Cordillera Blanca and Cordillera Huaytapallana for the period 1972-2018, as well as identify potential meteorological drivers of these changes in order to extend the mass balance record back in time and understand the long-term regional causes of glacial recession. In order to do this Landsat imagery is used to identify glaciers, alongside repeat DEMs derived from satellite altimetry and historic maps. DEMS are used to measure glacier surface elevation changes and calculate mass balance. Comparisons with time-series of meteorological data are conducted to identify potential forcing factors of glacial mass balance. The results of this study show that the glaciers of CB (-0.45 ± 0.08 m yr^{-1} w.e) and CH (-0.48±0.12 m yr^{-1} w.e) have undergone substantial mass loss over the last 50 years. Variations in mass balance are observed based on glacier aspect and elevation, as well as over the different time periods studied. Meteorological analysis identifies precipitation phase and humidity to be the main forcing factors of Cordillera Blanca mass balance, with air temperature and precipitation phase important for the Cordillera Huaytapallana.

1. Introduction

With a combined ice-covered area of 2,560 km^2, the Andes contain more than 99% of the world's tropical glaciers (Dyurgerov and Meier, 2005; WGI, 1989). These glaciers are sensitive indicators of both regional and global climate change (Francou et al., 2005; Hastenrath, 1994; Kaser and Georges, 1999; Lemke et al., 2007) and provide an important water source for downstream communities, buffering dry season discharge variability (Vergara et al., 2007; Vuille et al., 2008b, 2018). Tropical glaciers have lost mass over the last several decades (Francou and Vincent, 2017; Rabatel et al., 2013; Vuille et al., 2008a), and despite some glaciers experiencing brief periods of mass gain, the average trend in mass balance from field measurements has been negative for much of the last 50 years (Rabatel et al., 2013). Rabatel et al., (2013) show that the overall rate of mass loss has decreased in recent years, with a mass balance of -0.2 m yr^{-1} water equivalent (w.e) from 1964-1975 decreasing to -0.76 m yr^{-1} w.e from 1976-2010. Recent Peruvian measurements indicate a mass balance of between -0.01 ± 0.14 and -0.34±0.08 m yr^{-1} w.e for the period 2000-2013 (Braun et al., 2019). Other studies have found a more negative mass balance, with Dussaillant et al., (2019) measuring an overall Andean mass balance of −0.72 ± 0.22 m yr^{-1} w.e from 2000-2018. Losses are most pronounced at smaller and lower altitude glaciers (Rabatel et al., 2013; Veettil et al., 2017), and as a result, it has been suggested that low altitude Andean glaciers may be entirely lost by 2050-2090 (Vuille et al., 2008a). Other predictions indicate that by 2100 the tropical Andes may be ice free below ~6000 m a.s.l (Drenkhan et al., 2018; Schauwecker et al., 2017).

Glacial recession in the tropical Andes has previously been linked to large-scale climatic changes (Bury et al., 2011; Mark et al., 2010; Lynch, 2012). Vuille et al., (2008a) report an overall tropical

Andean warming of 0.10°C per decade over the 70 years prior. Vuille and Bradley (2000) identify a warming of 0.11°C per decade from 1939-1998, with the 1973-1998 warming being 0.32-0.34°C per decade. Studies of both the Cordillera Blanca and Huaytapallana identify similar local trends in temperature (Schauwecker et al., (2014) Mark and Seltzer, (2005) (Veettil et al., 2018)). Overall, a significant warming trend is found across the 20th century. Temperature is important with respect to glaciers both by directly driving ablation and as a control on precipitation phase, which in turn affects surface albedo and net surface shortwave radiation at the glacier surface (Schauwecker et al., 2014).

Humidity is another significant climatic factor for tropical glaciers as it controls the balance between ice sublimation and melting. The greater energy requirements of sublimation mean that an increase in sublimation results in a decrease in mass loss. (Mark and Seltzer, 2005; Vuille et al., 2003; Wagnon et al., 1999a, 1999b). Humidity is also related to cloud cover and precipitation which are significant for mass balance (Vuille et al., 2003). Humidity has increased in the Cordilleras Blanca and Huaytapallana over the 20th and 21st centuries (Vuille et al., 2003; Veettil et al., 2018). Changes in precipitation are significant for tropical mass balance as they represent the largest driver of inter-annual mass balance variability (Vuille et al., 2008b) however the historical record is poorly documented in Peru (Rabatel et al., 2013). A weak precipitation increase for Northern Peru is identified for 1950-1994 with a small increase observed at high altitudes (Vuille et al., 2003). Mark and Seltzer, (2005) used 1953-1998 data and found no significant changes in high altitude precipitation in the Peruvian Andes. Schauwecker et al., (2014) identified a 60 mm per decade increase in Cordillera Blanca precipitation from 1983-2012. A large increase occurs until 1993, after which precipitation levels remain consistent but above pre-1993 levels (Schauwecker et al., 2014).

To date, multidecadal field-based observations of glacier mass balance in the Peruvian Andes are limited in number, spatial extent and representivity. Similarly, comprehensive cordillera-wide assessments of glacier volume loss and geodetic mass balance are limited to recent decades (>20 yr), precluding their use in assessment of regional-scale glacier-climate interactions. This paper uses digitised legacy cartographic products in combination with modern remote sensing observations of glacier surface elevation to investigate spatially resolved multidecadal (>50 years) glacier mass balance and climate linkages for two major Andean glaciated regions, the Cordilleras Blanca and Huaytapallana, Peru. It is important to study Andean glacier-climate interactions to understand forcing factors and to predict how future climate change may affect glacier volumes and water resources for downstream users in years to come.

2. Study Site

The Cordillera Blanca (Fig 1a) contains around one quarter of all tropical glaciers (Kaser et al., 2003), covering a total glaciated area of 449 ± 56 km^2 (Silverio and Jaquet, 2017). These glaciers drain into the Rio Santa catchment through ten tributary rivers with catchment areas from 41 to 384 km^2 (Burns and Nolin, 2014). The Cordillera Huaytapallana (Fig 1b) is a smaller glaciated region with glaciers covering an area of 12.65 km^2 (Veettil et al., 2018). These glaciers provide crucial water supply to the Rio Shullcas and for consumption and agriculture for the city of Huancayo and the surrounding region (Mark et al., 2017). The glaciers of both regions are steep and heavily crevassed (Veettil et al., 2018). Located in the outer tropics, both cordilleras have a dry season centred on the austral summer (JJA) and a wet season covering the rest of the year (Schauwecker et al., 2014).

Monitoring of these glaciers is essential as they provide a crucial source of water for local communities (Crumley, 2015; Kaser et al., 2003). This is particularly pertinent for rural communities which rely on glacial meltwater for various economic activities and subsistence agriculture (Mark et al., 2017). In general, tropical glaciers act as a store of water and supplement river discharge during the dry season (Kaser et al., 2003; Milner et al., 2017). Glacial recession can cause an initial increase in discharge, followed by a sharp decline, a concept known as peak water (Baraer et al., 2012; Carey et al., 2014; Chevallier et al., 2011). The Cordillera Blanca represents a significant water source for the Rio Santa, and as such disruption to this hydrological regime could be extremely damaging to ecology, human livelihoods, industry and agriculture within the basin. The importance of glacial meltwater varies by sub-catchment, with discharge being more heavily reliant on glacial inputs in catchments with a higher percentage glacier cover (Kaser et al., 2003). Any decreases in the glacial component of discharge will also put increased pressure on other water sources. Decreasing glacial area is projected to result in groundwater forming a larger percentage of dry season discharge (Glas et al., 2018; Vuille et al., 2008a, 2008b,) which is likely to place greater strain on groundwater reserves. The increased reliance of discharge on precipitation and groundwater will increase the seasonality of discharge regimes and has the potential to increase the risk of drought impacts on a multi-year scale (Baraer et al., 2009; Mackay et al., 2020). The impact of declining water availability is already affecting Andean communities (Bury et al., 2011; Crumley, 2015; Mark et al., 2010), with water supply essential for agriculture, urban usage, industry, mining and hydropower (Condom et al., 2012). Declining water availability is not solely driven by reductions in supply, increases in water demand from growing urban centres also impact available water supplies (Bury et al., 2011). Reductions in water availability are not spatially or temporally uniform (Mark et al., 2017), and as a result the allocation of water rights presents a complex regional political issue (Rasmussen, 2017), with allocation often focussing on the needs of downstream users rather than upstream communities (Lynch, 2012).

Hydropower forms around 80% of Peru's electricity generation capacity, however this is projected to be significantly impacted by glacial recession (Vergara et al., 2007). The Cordillera Blanca contains the Canon del Pato facility; the third largest hydroelectric plant in Peru which supplies ~10% of national hydropower generation capacity (Mark et al., 2010). Reductions in discharge as a result of glacial recession could therefore present a significant energy issue in the region. This power generation is also significant source of energy for mining operations which form a large part of the regional economy. Estimates from 2009 found that 41% of the Rio Santa catchment is covered by mining concessions with this in turn forming 40% of all economic production from the region (Bebbington and Bury, 2009). Mining itself is also a substantial water user (Mark et al., 2017) and as such a reduction in water availability due to glacial recession could be place a significant additional economic burden on the region.

Much of the Cordillera Blanca falls within the boundaries of the Huascarán National Park, a UNESCO world heritage site (Lipton, 2014), and therefore an important conservation region. The high mountains of the Peruvian Andes are also known to comprise a highly biodiverse ecosystem (Mark et al., 2017). Such ecosystems rely on the glaciers and the waters they provide and therefore glacier loss presents a significant threat. This is particularly true of the wetlands found in the valleys of the Cordillera Blanca with these projected to substantially decrease in size as glacier area decreases (Polk et al., 2017). A loss of wetlands would be significant for the food and water security of rural communities as they buffer dry season river flows (Baraer et al., 2009) and provide a source of high quality livestock feed (Mark et al., 2017).

Extending the record of glacial mass balance back in time is important in order to understand the long-term regional causes of glacial recession. An understanding of historical mass balance and the associated causes is also important for future projections of glacier and hydrological change. This study uses historical mapping and satellite imagery in order to quantify historic changes in glacial mass balance for the Cordillera Blanca and Cordillera Huaytapallana. The meteorological forcing factors of these changes in mass balance are also investigated.

3. Methodology

3.1 Data Acquisition and Processing

In order to quantify historic mass balance, repeat elevation and glacial area measurements are required. In this study we used elevation data reconstructed from historic mapping, as well as 21st century satellite-based measurements to create a consistent, spatially-resolved record of glacier elevation changes from 1972 to 2015. Historic satellite imagery was also used to quantify changes in glacier area. Elevation and area changes were then combined to calculate the geodetic mass balance. The historic record of mass balance was then compared against local meteorological data in order to investigate the forcing factors behind glacial change.

Landsat Thematic Mapper (TM) and Operational Land Imager (OLI) imagery were used for glacier mapping due to their relatively high spatial resolution (30 m) and long historic record (1973-present) (Chander et al., 2009). Details of the scenes used in this work are provided in Table 1. Landsat imagery also has the spectral resolution and band differentiation required to compute a normalised difference snow index (NDSI) (Burns and Nolin, 2014; Silverio and Jaquet, 2017) [Glacier areas for 1972 could not be mapped as Landsat MSS imagery available for this time lacks the bands required to compute an NDSI]. For all other years, images were obtained from the end of the dry season (August or September) to minimise snow cover and therefore classification errors. Images were chosen from years as close as possible to the date of digital elevation data, while minimising cloud cover. These were converted from digital numbers (DN) to top of atmosphere (TOA) reflectance following the methods outlined by Chander et al., (2009) and USGS, (2018, 2019), to improve the performance of the index (Burns and Nolin, 2014; Seehaus et al., 2019). This also enhances inter-scene comparability under varying illumination conditions (Burns and Nolin, 2014), allowing a single threshold value to be used for analysis.

1972 Elevation data were obtained from the Instituto Geográfico Nacional (IGN) 1:100,000 Cartas Nacionales del Perú, available as pre-digitised 50 m contour maps. These were interpolated to a 30 m resolution DEM using ArcGIS Topo to Raster tools. 1986 elevation data were obtained from 1:500,000-scale United States Airforce (USAF) Tactical Pilotage Charts, with a contour interval of 500 feet (~152 m), the accuracy of these contours is given as ±9 m (Military Specification [MIL]-T-89101(DMA)). Contours were hand digitised and interpolated to a 30 m DEM. 2000 elevation data were acquired from the NASA Shuttle Radar Topography Mission (SRTM) 1 arc-second void-filled data product, as it is accurate in high mountain areas, with a mean difference from reference data of ±7 m (Frey and Paul, 2012). Unlike ASTER GDEM data, SRTM data has a precise date (Frey and Paul, 2012). 2018 elevation data were derived from photogrammetric processing of ASTER stereo image pairs, and provided in the form of 2000-2018 elevation changes, differenced from SRTM data (Dussaillant et al., 2019). As such, 2018 surface elevations were reconstructed by multiplying the yearly changes by 18 and adding these to the SRTM elevations.

Meteorological data were obtained from SENAMHI (National Service of Meteorology and Hydrology of Peru) for the Recuay and Huayao stations in the Cordilleras Blanca and Huaytapallana respectively (see Figure 1). These stations were chosen for the meteorological variables recorded and their records covering the entire study period. Where gaps were present they were infilled using linear regression between the chosen station and another proximal meteorological station (Heydari and Khalifeloo, 2015; Ramos-Calzado et al., 2008). Where gaps could not be filled with data from an alternative station, infilling was conducted by taking the average of the variable on the same day two years before and after the missing date. Meteorological data were available to 2017 and therefore this analysis is limited to the period 1972-2017 only.

Temperature data were provided as daily maximum ($Temp_{max}$)(°C) and minimum ($Temp_{min}$)(°C) values. Precipitation data were provided as either twelve or six hourly precipitation totals, with observation lengths and times. To achieve consistency across the record, the values were converted to daily totals ($Precip_{total}$) (mm) by summing the values for each given 24-hour period. Dry (T_d) (°C) and wet bulb (T_w) (°C) temperatures were recorded at 7am, 1pm and 7pm. Absolute humidity at 7am (AH_{7am}) (kgm^{-3}), 1pm (AH_{1pm}) (kgm^{-3}) and 7pm (AH_{7pm}) (kgm^{-3}) was calculated from the wet and dry bulb temperatures in order to find atmospheric moisture content without the influence of temperature on humidity. Firstly, wet bulb saturation vapour pressure, E_w(mb) was calculated as;

$$E_w = 6.108e^{\frac{17.27T_w}{273.3+T_w}} \tag{1}$$

Partial water vapour pressure, E (mb), was then found;

$$E = E_w - 0.00066T_pP(1 + 0.00115T_w) \tag{2}$$

Where T_p (°C) is the wet bulb depression;

$$T_p = (T_d - T_w) \tag{3}$$

and P is barometric pressure (mb). P was assumed constant and based on station altitude ,Z (Dewpoint, n.d.; Vaisala Oyj, 2013);

$$P = 101.3\frac{293 - (0.065Z)^{5.26}}{293} \tag{4}$$

Absolute humidity (AH) (kg m^{-3}) was calculated using the R package 'humidity' (Cai, 2018). Which uses the following formula, where R_v is the specific gas constant for water vapour;

$$\mathrm{AH} = \frac{E}{R_vT_d} \tag{5}$$

3.2 Glacier Area Delineation

Glacier areas were automatically-delineated from Landsat imagery using NDSI and a threshold of ≥0.42; chosen as this has previously been shown to accurately discriminate glacier ice from the surrounding terrain in this region (Burns and Nolin, 2014). The NDSI was calculated using TM and OLI band information as:

$$\frac{\mathrm{TM}_2 - \mathrm{TM}_5}{\mathrm{TM}_2 + \mathrm{TM}_5} \tag{6a}$$

OR

$$\frac{\mathrm{OLI}_3 - \mathrm{OLI}_6}{\mathrm{OLI}_3 + \mathrm{OLI}_6}. \tag{6b}$$

Topographic shadowing resulted in some classification errors, which were resolved using additional Landsat scenes with different solar elevation angles to identify and remove shadowed areas. Misclassifications also occurred as a result of water bodies. To resolve this, lake areas were manually delineated and clipped from the NDSI output areas. Obscuring of glacier areas by cloud was resolved using temporally proximate imagery to manually correct glacier outlines. Glaciers smaller than 0.01 km^2 were removed as these do not meet the definition of glacier used here (Burns and Nolin, 2014). Debris-covered glaciers were not included as they are considered to form only a very small proportion of the total ice-covered area in the region (Burns and Nolin, 2014).

As a globally-complete glacier inventory dataset, the Randolph Glacier Inventory (RGI, Pfeffer et al., 2014; Arendt et al., 2015) covers both the Cordilleras Blanca and Huaytapallana and was used here to divide total ice areas measured by NDSI into individual glacier basins. This was done by taking the glaciers identified by the RGI and projecting their outlines outwards so that they cover the entire area measured in this study. This provides a good approximation for the locations of glaciers and therefore allows analysis of individual glaciers to be undertaken.

Peruvian glacier area changes have previously been shown to vary based on elevation and aspect (e.g. Burns and Nolin, 2014; Kaser and Georges, 1997; Silverio and Jaquet, 2017; Veettil et al., 2018). In order to investigate these changes, all mapped glaciers for each Cordillera were divided based on their aspect and elevation characteristics. Altitudinal classification was conducted by creating 250 m altitudinal bands using SRTM data, starting from 4000 m a.s.l for the Cordillera Blanca and 4500 m a.s.l for the Cordillera Huaytapallana, up to the band which contained the highest glaciated peaks. This does not consider changes in elevation between time periods, but for ease of identifying altitudinal trends the method was deemed suitable. The aspect of each SRTM pixel was also found and grouped into the eight primary compass directions. This method does not consider the average glacier aspect but instead the aspect of individual glacier pixels. This means DEM artefacts could result in erroneous aspects but this is not considered likely to have a substantial effect on this analysis.

In order to measure the error in glacial area a plus/minus one pixel buffer around the NDSI measured area was taken, the average difference of these from the measures area was then taken as the error for an individual year (Burns and Nolin, 2014) using the following formula:

$$\sigma_{Area} = \frac{|A - A_{Plus}| + |A - A_{Minus}|}{2} \tag{7}$$

The various glacial divisions were then also conducted on these plus/minus buffered areas to estimate the error in each of these scenarios.

3.3 Geodetic Mass Balance Calculation

Area-averaged mass balance, $\dot{b}$ (m yr^{-1} w.e.) was calculated by solving the density-corrected volume balance using surface elevation changes and glacier areas (e.g. Barrand et al., 2010; Berthier et al., 2010), and following the notation provided by Arendt et al. (2006). First, surface elevation changes, Δh (m) were calculated by differencing the DEMs from the start and end of the chosen period.

$$\Delta h = DEM_{End} - DEM_{Start} \tag{8}$$

Mean surface elevation change, dh (m) was then calculated

$$dh = \sum_{A} \Delta h_i \tag{9}$$

Where Δh_i is the elevation change of an individual pixel and A is the glacier surface in which the pixels are contained. Total volume change, B, (m^3) was then calculated

$$B = dh \times {l_p}^2 \tag{10}$$

Where l_p is the side length of a pixel. The area-averaged net geodetic balance rate (mass balance, $\dot{b}$) was then calculated by multiplying B by the ratio of the density of ice to water (p, 850 ± 60 kg m^3; Huss, 2013), dividing by the number of years between observations (t), and dividing by the average of the glacier areas at the start and end of the measurement period (Arendt et al., 2006; Barrand et al., 2010).

To quantify uncertainties in mass balance, elevation change errors must first be measured. DEM error, σ_{DEM}, was measured as the standard deviation of height changes between each DEM and the reference SRTM DEM for stable non-ice terrain. Mean surface elevation change error, E_{dh}, was calculated as :

$$E_{dh} = \frac{\sqrt{{\sigma_{DEM_{Start}}}^2 + {\sigma_{DEM_{End}}}^2}}{\sqrt{n}} \tag{11}$$

Where n is the number of glacier pixels (Barrand et al., 2010). Average area error, E_A, was then found by:

$$E_A = \sqrt{{\sigma_{Area_{Start}}}^2 + {\sigma_{Area_{End}}}^2} \tag{12}$$

The volume to mass conversion error, E_ρ, was taken as 0.06 (Huss, 2013), except where the measured mass balance was less than 0.2 m yr^{-1} w.e. In this case a higher E_ρ of 0.30 was used to account for higher volume-mass conversion uncertainty in small mass balances (Braun et al., 2019; Huss, 2013; Seehaus et al., 2019). Volume change error, E_B, was then calculated using the following equation:

$$E_B = E_{dh} \times n \times {l_p}^2 \tag{13}$$

Standard error theory was then used to combine errors in density and volume change (Farías-Barahona et al., 2019; Malz et al., 2018) and calculate geodetic balance rate error, $E_{\dot{B}}$ by:

$$E_{\dot{B}} = \frac{\dot{B}\sqrt{\left(\frac{E_B}{B}\right)^2 + \left(\frac{E_\rho}{\rho}\right)^2}}{t} \tag{14}$$

Where t is the number of years between observations. Using equations 12 and 14 geodetic mass balance error, $E_{\dot{b}}$, was found by:

$$E_{\dot{b}} = \dot{b}\sqrt{\left(\frac{E_{\dot{B}}}{\dot{B}}\right)^2 + \left(\frac{E_A}{A}\right)^2} \tag{15}$$

3.4 Meteorological Analysis

To remove seasonal cycles and daily variation and allow for identification of long-term trends, yearly meteorological means (totals for precipitation) were calculated. To investigate the impact of meteorological changes on mass balance multiple linear regression was conducted between cumulative mass balance, AH_{7am}, AH_{1pm}, AH_{7pm}, $Temp_{max}$ and $Temp_{min}$. Model selection and averaging was used to identify the most predictive variables (Zuur et al., 2007), and assess which factors may be forcing glacial changes. Cumulative mass balance was calculated by assuming a linear change in mass for each of the periods studied. This however means any glacial fluctuations within these periods cannot be accounted for.

4. Results

4.1. Ice Surface Elevation Change

Cordillera Blanca elevation changes from 1972 to 2018 are characterised by high spatial variability and marked elevation dependence of glacier thinning (lowest elevation regions have the greatest thinning rates, Fig 2a). The majority of regions with an ice losses <5 m yr^{-1} are located at the terminus of lower elevation glaciers. Higher elevation regions, including glaciated mountain peaks and high plateaus, have positive or less strongly negative elevation changes. A small number of areas at high elevations have strongly positive elevation changes (1-4 m yr^{-1}). These rates of change are likely to be less accurate as a result of void filling or spatially-inconsistent uncertainties in 1972 maps.

An aspect-based variation in surface elevation change can also be seen with more negative elevation changes on north facing slopes and subsequently more positive on south facing slopes, as expected for southern hemisphere ice masses. There is also a change in the response of mass balance to elevation across different aspects. In the Cordillera Blanca this results in negative elevation changes occurring at higher elevations on the north facing slopes, with less negative/positive elevation changes at equivalent elevations on south-facing slopes.

Elevation changes for the Cordillera Huaytapallana are shown in Figure 2b. Elevation change rate variation with glacier elevation in the Cordillera Huaytapallana is similar in magnitude and spatial variability to the Cordillera Blanca (Fig 2a). In general, the lowest elevation areas have the most negative elevation changes, with the most significant losses being on the snouts of glaciers, as is seen for the Cordillera Blanca. The Cordillera Huaytapallana also has a very slight aspect-based trend in elevation changes. It can be seen in Figure 2b that north and east facing areas have slightly more negative surface elevation change than south and west facing areas. This also results in a similar combined pattern of elevation and aspect to the Cordillera Blanca, with the transition between surface elevation loss and surface elevation gain occurring at lower altitudes on south and west facing slopes.

When considering the elevation change of individual glaciers rather than the ice masses of the Cordillera Blanca as a whole (Fig 3a) a similar pattern is observed with glaciers with northerly aspects, and those with located at lower elevations, undergoing larger thinning rates than higher elevation areas and southerly-tending slopes. Some notable exceptions to this pattern exist, these include some of the smallest, lowest elevation glaciers which have disappeared entirely over the period analysed, as such rates of thinning may be misleading where the elevation has not been changing for a period of time owing to there being no ice present.

Similar to overall elevation change, analysis of the individual glaciers elevation change for the Cordillera Huaytapallana (Fig 3b) reveals that the lowest elevation glaciers have the most significant elevation losses. North and east facing glaciers also have a more significant elevation loss than those facing south and west, with the latter group having some glaciers with an overall elevation gain.

4.2 Mass Balance

Cordillera Blanca mass balance was negative for the period 1972-2018 (-0.45 ± 0.08 m yr^{-1} w.e). Across each of the individual periods mass balance remains similar (1972-1986; -0.44±0.07, 1986-2000; -0.58±0.11, 2000-2018; -0.33±0.07 m yr^{-1} w.e), indicating no acceleration in glacier loss in recent years. Cordillera Huaytapallana mass balance is similarly negative over the overall study period (-0.48±0.12 m yr^{-1} w.e). However, unlike the Cordillera Blanca there is a more significant variation in mass balance over time. Initially Huaytapallana mass balance is strongly negative, -1.20±0.27 m yr^{-1} w.e, from 1972-1986. This is followed by a positive period of mass balance from 1986-2000, 0.28±0.07m yr^{-1} w.e. from 2000-2018 mass balance returns to a negative phase (-0.32±0.09 m yr^{-1} w.e.).

From 1972-2018 Cordillera Blanca individual glaciers mass balances display a typical relationship with altitude for tropical glaciers (Kaser and Georges, 1999) (Fig 4a). This means the most negative mass balances occur at the lowest elevations (-3.75±4.07 m yr^{-1} w.e.), this then decreases linearly up to 5000-5250 m a.s.l. After this point mass balance remains consistently around -0.3 m yr^{-1} w.e. From 1972-1986 a non-linear relationship between mass balance and altitude is found. For this period a weakly positive mass balance is found at the lowest altitudes with this switching to an increasing negative mass balance for glaciers at elevations greater than 5000 m a.s.l level. From 1986-2000 this trend reverses. In this period, strongly negative mass balances are found at the lowest altitudes, with a positive mass balance found above 5500 m a.s.l. For the 2000-2018 period mass balances are negative at all altitudes with the most negative mass balances occuring at the lowest altitudes, decreasing up to 5000-5250 m a.s.l band, after which they remain relatively constant between -0.20 and -0.28 m yr^{-1} w.e..

Cordillera Blanca mass balance is also observed to vary depending on glacier aspect. Analysis from 1972-2018 found mass balance to be negative across all aspects, varying from most negative on north-westerly slopes (-0.63±0.14 m yr^{-1} w.e.) to least negative on south-easterly aspects (-0.25±0.06 m yr^{-1} w.e.). The overall trend then shows that north facing regions have more negative mass balances than south tending slopes. 1972-1986 mass balances vary similarly to the overall record, with strongly negative mass balances found on northerly tending aspects. From 1972-1986 a positive mass balance is recorded for south facing regions of the Cordillera Blanca. 1986-2000 shows a complete trend reversal compared to 1972-1986. From 2000 to 2018 mass balance is consistently negative across all aspects.

Cordillera Huaytapallana mass balance variation with altitude (Fig 4b) from 1972-2018 is similar to that observed for the Cordillera Blanca, the most negative glacier mass balances are found at the lowest altitudes (-1.71±2.03 myr^{-1} w.e. at 4500-4750 m a.s.l) with mass balance gradually becoming less negative for glaciers at higher altitudes. From 1972-1986 this trend is reversed, with positive mass balances at the lowest altitudes, above 5000 m a.s.l mass balance becomes increasingly negative. From 1986 to 2000 negative mass balances are again found at the lowest altitudes, however in this case mass balances are positive above 5000 m a.s.l. 2000-2018 mass balance varies with altitude in the same fashion as the 1972-2018 trend, albeit with more negative mass balance found at the highest altitudes. Cordillera Huaytapallana mass balance varies very little by aspect, with significant overlap between the error bars across all aspects. 1972-1986 shows a similar trend to 1972-2018, with little variation present. While 1986-2000 shows near balance except on west tending slopes where positive mass balance is observed. Unlike other periods, 2000-2018 has a more substantial trend in mass balance with aspect. South tending aspects have a less negative mass balance than all other aspects.

5. Discussion

5.1 Spatial Variability in Geodetic Mass Balance

The Cordillera Blanca spatial variability in mass balance closely reflects the pattern of negative mass balance at low altitudes with the rate of mass loss decreasing with increasing altitude that is typically observed for tropical glaciers (Burns and Nolin, 2014; Hanshaw and Bookhagen, 2014; Rabatel et al., 2013; Silverio and Jaquet, 2017; Seehaus et al., 2019; Veettil, 2018). 1986-2000 and 2000-2018 results in this study show an altitudinal trend similar to the typically measured trends while 1972-1986 shows an inverse trend with a negative mass balance at the highest elevations and a positive or less negative mass balance at lower elevations. Aspect-based variations of mass balance show the most negative mass balances to be found on northerly aspects, with mass balance being less negative towards the south. These results support the findings of Kaser and Georges, (1997), Racoviteanu et al., (2008) and Veettil, (2018). However they are contrary to the findings of Mark and Seltzer (2005); their results however may not be comparable as the only south-west facing glacier they study is Queshque Main which experienced a substantial surface lowering in both this study and theirs. The cause of the reversal of the aspect-based trend from 1986-2000 relative to the other time periods is not clear. The spatial coherence between elevation changes from 1972-1986 and 1986-2000 however indicate that this may be the result of unquantified DEM uncertainties. However, similar patterns of change with altitude are observed for the Cordillera Huaytapallana, with 1972-1986 being the only period to reveal a mass balance trend with altitude that significantly deviates from the expected pattern.

The unusual altitudinal pattern of mass balance from 1972-1986 is considered likely to be a result of uncertainties in the historic mapping, most likely in the 1986 elevation data set, owing to the fact that the 1972-2018 altitudinal pattern of mass balance is more typical of tropical glaciers. Despite analysis of non-ice elevations, higher-elevation uncertainties from 1972 and 1986 historic maps may be difficult to fully quantify. Adalgeirsdóttir et al., (1998) documented a greater error in glacier elevations at higher elevations when analysing Alaskan historic contour maps. This is due to the difficulty in identifying features in stereoscopic imagery in featureless high elevation accumulation zones. These errors may be present in the historic maps used in this study, however in order to confirm this, comparisons would need to be made with raw air photo images or independent datasets from the time, neither of which are available. It is notable that while larger mass balance errors are found at lower altitudes, this is a result of the fact majority of the glacier termini are in the lowest altitude bands and as such the 1-pixel buffer used for area error calculations estimates a large error in the lowest altitude bands. Conversely high-altitude areas have lower estimated error in glacial area as much of these bands are almost entirely covered in ice. These low altitude errors may also be overstated as the 1-pixel buffer method has been previously shown to over-estimate error (Hoffman et al., 2007).

A significant feature that can be observed from individual Cordillera Blanca glacier mass balances is the fact that glaciers further south tend to have much less negative or even positive mass balances. This supports the findings of Kaser et al. (2003) with southern portions of the Cordillera Blanca having less negative mass balances due to north-south meteorological gradients. The northern Cordillera Blanca valleys receive greater precipitation than southern ones (Vuille et al., 2008a, 2008b). Kaser et al. (2003) also suggest that variation in mass balance may be due to the smaller altitudinal range of the southern glaciers.

5.2 Context of Previous Findings

Kaser et al., (2003, fig.8a) report Cordillera Blanca mass balance from 1972-1986 of -0.5 m yr^{-1} w.e., a value similar within error bounds to the -0.44±0.07 m yr^{-1} w.e reported for the same period in this study. For the area defined by Seehaus et al. (2019) as R1 (containing the Cordillera Blanca and the Cordillera Huaytapallana) 2000-2016 mass balance is measured as -0.21±0.11 m yr^{-1} w.e. The 2000-2018 mass balance in this study, -0.45±0.09 m yr^{-1} w.e (Cordillera Blanca) and -0.32±0.10 m yr^{-1} w.e. (Cordillera Huaytapallana), are similar to the values found by Seehaus et al., (2019) albeit slightly more negative; this provides a good level of confidence to the results of this study. Cordillera Blanca surface elevation change rates from 1962-2008 in Huh et al., (2017) are between -0.207 m yr^{-1} and -1.393 m yr^{-1}. In comparison the Cordillera Blanca mean surface elevation changes in this study are -0.56 m yr^{-1} for 1972-2000 and -0.48 m yr^{-1} for 1972-2018. These values are at the lower end of those provided by Huh et al. (2017), presumably due to the inclusion of high altitude glaciers in the study that are not measured by Huh et al. (2017). No Cordillera Blanca mass balance measurements are available in the literature for 1986-2000, however Burns and Nolin, (2014) measure an area change of -161 km^2 from 1987-2000, indicating a likely negative mass balance trend.

Besides Seehaus et al. (2019) no studies of Cordillera Huaytapallana mass balance were available for comparison. López-Moreno et al., (2014) and Veettil et al., (2018) measured area changes of -11.6 km^2 and -12.14 km^2 for 1984-2011 and 1985-2015 respectively. Again, these results support the overall negative Cordillera Huaytapallana mass balances observed in this study.

5.3 Meteorological Drivers

Temperature trends in both study regions show that minimum temperatures for both Cordilleras have increased at a rate of 0.098 °C per decade (Cordillera Blanca $p=0.9$, Cordillera Huaytapallana $p=0.06$), meanwhile Cordillera Blanca maximum temperature remains unchanged (Figure 5). Cordillera Huaytapallana maximum temperatures have increased at a rate of 0.31°C per decade ($p<0.001$). Precipitation in the Cordillera Blanca has increased by 93 mm per decade ($p=0.001$) along with an increase in the total number of dry days (Figure 5). Together this indicates that the increase in total precipitation is a result of more intense precipitation events. No significant changes in precipitation were observed for the Cordillera Huaytapallana. Trends in humidity were also analysed for both Cordilleras (Fig 6). Statistically significant increases in 7am, 1pm and 7pm humidity were observed for the Cordillera Blanca, with the largest increases occurring after 2003. 7am humidity for the Cordillera Huaytapallana increased at a rate of 0.00011 kgm^{-3} per decade ($p<0.001$) from 1972-2017.. However no significant trend was observed in 1pm or 7pm humidity, despite this there is some substantial variability in Cordillera Huaytapallana humidity in the last 50 years, as can be seen in figure 6.

Comparison of meteorological parameters and cumulative mass balance are presented in figures 6-13. Figure 6a shows that a rise in Cordillera Blanca precipitation from 1972-2017 coincides with a period of negative mass balance. Similarly, the previously described rise in minimum temperature occurs across the same period. From 1986-2000 the most negative Cordillera Blanca mass balance was observed, figure 6.b shows that this coincides with a period of higher, but declining, maximum temperatures. Comparing mass balance to humidity reveals no obvious relationships.

A differing relationship between mass balance and meteorological parameters is observed above and below 5250 m a.s.l (Figures 7-8). Above 5250 m a.s.l mass balance and maximum temperature appear closely related (Fig 7.a), with negative mass balances occuring as maximum temperatures rise (1972-1986, 2000-2017) and positive mass balances occuring alongside declining maximum temperature (1986-2000). This indicates that above 5250 m a.s.l glacier mass loss is primarily influenced by temperature induced melting. Below 5250 m a.s.l the primary control on mass balance appears to be humidity. The relationship between mass balance and humidity is seen most clearly for AH_{7am} and AH_{7pm} (Fig 8.d, f). A positive low altitude mass balance is found from 1972-1986, alongside a period of decreasing humidity. From 1986-2017 humidity increases with mass balance negative. This indicates that humidity is controlling the balance between sublimation and melting at the glacier surface. This is due to increases in humidity resulting in increased melting and therefore greater mass loss as a result of the lower energy requirement of melting to change the phase of a given volume of ice, relative to sublimation (Mark and Seltzer, 2005; Vuille et al., 2003; Wagnon et al., 1999a, 1999b). Post-2000 a relationship between humidity and mass balance similar to that of AH_{7am} and AH_{7pm} is found between AH_{1pm} and mass balance. Prior to 2000 little change is observed in AH_{1pm}. This indicates that night-time humidity changes may have been more significant as a driver of glacial change than daytime humidity changes prior to 2000. Below 5250 m a.s.l the 1972-2017 mass balance trend is negative, alongside overall rises in both precipitation and minimum temperature. This suggests that precipitation below this elevation may be falling more frequently as rain rather than snow, controlling surface albedo and increasing surface melting, resulting in the negative mass balance observed (Gurgiser et al., 2013).

Aspect based variations in the relationships between Cordillera Blanca mass balance and meteorology are also observed (Figures 9-10). Northern facing slopes have an inverse relationship between mass balance and maximum temperature (Figure 9.b) with periods of rising (1972-1986, 2000-2017) (falling, 1986-2000) temperature coinciding with negative (positive) mass balance. This relationship is not found on other aspects and may be due to the close correlation between incident solar radiation and temperature, with higher solar radiation totals found on northern Cordillera Blanca slopes than southern ones (Mark and Seltzer, 2005). Southerly aspects are more closely related to humidity, with rises (falls) in humidity coinciding with negative (positive) mass balance (Figure 10.d-f). Like the mass balance-humidity relationship below 5250 m a.s.l, southerly mass balance is most closely related to AH_{7am} and AH_{7pm}. On eastern and western facing aspects mass balance is consistently negative from 1972-2017. This correlates closely with the overall increases in both precipitation and minimum temperature, suggesting that, like low altitude portions of the Cordillera Blanca, changes in precipitation phase may be important in controlling mass balance on eastern and western slopes. Between 1972 and 1986 a strongly negative mass balance was observed on northern aspects alongside a rise in precipitation (Figure 9.a) with the inverse found on southern facing slopes (Figure 10.a). This indicates that solar radiation induced changes in precipitation phase may also be important in controlling mass balance. Further investigation into the changes in solar radiation incident at the glacier surface over time would be required to confirm this hypothesis.

Analysis of Cordillera Huaytapallana mass balance and meteorological trends (Figure 11), show that there is a close correlation between mass balance and maximum temperature (Figure 11.b), with periods of negative mass balance from 1972-1986 and 2000-2017 coinciding with significant rises in maximum temperature, while the positive mass balance between 1986-2000 occurs during a period of much smaller temperature increases. Additionally an inverse relationship between precipitation and mass balance is observed, with rising (falling) precipitation during periods of negative (positive) mass balance. Rising maximum and minimum temperatures alongside the precipitation relationship indicate that changes in precipitation phase and atmospheric warming are the main factors forcing Cordillera Huaytapallana mass balance.

Like the Cordillera Blanca, the Cordillera Huaytapallana exhibits different relationships between mass balance and the measured meteorological parameters at different altitudes. Below 5000 m a.s.l Cordillera Huaytapallana mass balance appears to be closely related maximum temperature (Figure 12.b), with decreasing mass balance from 1972-2017 occuring alongside a rise in temperature. This indicates that low altitude mass loss is primarily driven by atmospheric warming. Additionally, changes in precipitation inducing changes in accumulation may be important with the most strongly negative mass balance occuring alongside a period of declining precipitation (1986-2000). Where precipitation increases (1972-1986, 2000-2017) mass balance is less negative. Above 5000 m a.s.l there appears to be little relationship between mass balance and the studied meteorological variables (Figure 13). This primarily relates to the fact that above 5000 m a.s.l Cordillera Huaytapallana glaciers have been relatively stable over the last 50 years. There is relatively little aspect-based variation in the relationship between Cordillera Huaytapallana mass balance and meteorology, with relationships between mass balance and maximum temperature/precipitation found on all aspects, as was observed for the Cordillera as a whole.

Only a single meteorological station was analysed for each Cordillera and therefore altitudinal and spatial meteorological gradients (Racoviteanu et al., 2008; Vuille and Bradley, 2000) are therefore not fully considered in this study. Elevation-based temperature gradients have also been shown to be different for eastern and western Cordillera Blanca slopes (Vuille and Bradley, 2000) adding a further parameter that is not considered in this study. Wind strength and frequency has also been shown to be a significant factor in controlling the mass balance of tropical glaciers (Favier et al., 2004) however the meteorological data available for this study did not allow for changes in wind strength to be analysed. It should also be noted that because only a small number of mass balance measurements are recorded short term fluctuations in glacier mass and their relationship with meteorological conditions are not able to be considered in this study. Despite these limitations the results presented in this study provide an insight into historic glacial fluctuations and their potential drivers.

6. Conclusions

This study presents a long-term (1972-2018), spatially-resolved mass balance record for the Cordilleras Blanca and Huaytapallana using elevation changes from reconstructed historic and contemporary satellite-based elevation data sources. Previous studies have focussed on shorter time periods and/or specific glaciers within these regions, but this study expands upon this previous work, quantifying long term changes in glaciers across the region. The Cordillera Blanca experienced a mass balance of -0.45 ± 0.08 m yr^{-1} w.e from 1972-2018 the period studied and the Cordillera Huaytapallana a mass balance of -0.48±0.12 m yr^{-1} w.e.. Mass balance was found to be more negative at low altitudes for both Cordilleras. For the Cordillera Blanca an aspect-based variation in mass balance was also observed, with more negative mass balances on north facing slopes than south. Comparison between cumulative geodetic mass balance and annual meteorological series was conducted to attempt to identify the causes of the observed glacial changes. This analysis revealed precipitation phase and humidity, controlling albedo and the balance between sublimation and melting respectively, have been the main factors forcing Cordillera Blanca mass balance, meanwhile Cordillera Huaytapallana mass balance has been primarily driven by changes in air temperature and precipitation phase.

The glacial mass losses observed in this study are expected to result in the catchments downstream of the studied glaciers becoming increasingly precipitation dominated. This could also result in a decrease in water availability for large-scale economic activities, as well as being significant for the lives of rural Andean communities. Future research should focus on: Changes in the mass balance of debris covered glaciers, which have been shown to be losing mass in the region (Wigmore and Mark, 2017). This was not investigated here due to the difficulty in automatically identifying debris covered glaciers. This could help further the understanding of elevation changes at low altitudes; High altitude meteorological changes to further investigate the forcing factors suggested in this study ; and, Sub-catchment hydrological changes (where data is available) to assess the impacts for rural water access of glacial decline on water resources at local scale.

These results show that there has been a significant loss in mass in the glaciers of the Cordilleras Blanca and Huytapallana over the last 50 years and that these changes have been driven by changes in the local climate. This is particularly significant given the importance of these glaciers as a water source for downstream communities. The research presented in this study shows that long term glacier loss has occurred in these Cordilleras and that given the meteorological forcing factors future climate change could result in further mass loss.

References

Adalgeirsdóttir, G., Echelmeyer, K.A. and Harrison, W.D. (1998) Elevation and volume changes on the Harding Icefield, Alaska. *Journal of Glaciology*, 44 (148): 570–582. doi:10.3189/S0022143000002082.

Arendt, A., Echelmeyer, K., Harrison, W., et al. (2006) Updated estimates of glacier volume changes in the western Chugach Mountains, Alaska, and a comparison of regional extrapolation methods:. *Journal of Geophysical Research: Earth Surface*, 111 (F3): n/a-n/a. doi:10.1029/2005JF000436.

Arendt, A., Tad Pfeffer, Anthony Arendt, Andrew Bliss, Tobias Bolch, Graham Cogley, Alex Gardner, Jon Ove Hagen, Regine Hock, Georg Kaser, Christian Kienholz, Evan Miles, Geir Moholdt, Nico Molg, Frank Paul, Valentina Radic, Phillipp Rastner, Raup, Justin Rich, Martin Sharp, L Andreasson, S Bajracharya, N Barrand, M Beedle, E Berthier, R Bhambir, I Brown, D Burgess, E Burgess, F Cawkwell, T Chinn, L Copland, N Cullen, B Davies, H De Angelis, A Fountain, H Frey, B Giffen, N Glasser, S Gurney, W Hagg, D Hall, U Haritashya, G Hartmann, S Herried, I Howat, H Jiskoot, T Kromova, A Klein, J Kohler, M Konig, D Kriegel, S Kutuzov, I Levrentiev, R Le Bris, Z Li, W Manley, C Mayer, B Menounos, A Mercer, P Mool, A Negrete, G Nosenko, C Nuth, A Osmonov, R Petterson, A Racoviteanu, R Ranzi, M Sarikaya, C Schneider, O Sigurdsson, P Sirguey, C Stokes, R Wheate, G Wolken, L Wu, F Wyatt (2015) Randolph Glacier Inventory – A Dataset of Global Glacier Outlines: Version 5.0., Global Land Ice Measurements from Space, Digital Media, Boulder, CO, USA.

Baraer, M., Mark, B.G., McKenzie, J.M., et al. (2012) Glacier recession and water resources in Peru's Cordillera Blanca. *Journal of Glaciology*, 58 (207): 134–150. doi:10.3189/2012JoG11J186.

Baraer, M., McKenzie, J.M., Mark, B.G., et al. (2009) Characterizing contributions of glacier melt and groundwater during the dry season in a poorly gauged catchment of the Cordillera Blanca (Peru). *Advances in Geosciences*, 22: 41-49. doi:10.5194/adgeo-22-41-2009.

Barrand, N.E., James, T.D. and Murray, T. (2010) Spatio-temporal variability in elevation changes of two high-Arctic valley glaciers. *Journal of Glaciology*, 56 (199): 771–780. doi:10.3189/002214310794457362.

Bebbington, A.J. and Bury, J.T. (2009) Institutional challenges for mining and sustainability in Peru. *Proceedings of the National Academy of Sciences*, 106 (41): 17296–17301. doi:10.1073/pnas.0906057106.

Berthier, E., Schiefer, E., Clarke, G.K.C., et al. (2010) Contribution of Alaskan glaciers to sea-level rise derived from satellite imagery. *Nature Geoscience*, 3 (2): 92–95. doi:10.1038/ngeo737.

Braun, M.H., Malz, P., Sommer, C., et al. (2019) Constraining glacier elevation and mass changes in South America. *Nature Climate Change*, 9 (2): 130–136. doi:10.1038/s41558-018-0375-7.

Burns, P. and Nolin, A. (2014) Using atmospherically-corrected Landsat imagery to measure glacier area change in the Cordillera Blanca, Peru from 1987 to 2010. *Remote Sensing of Environment*, 140: 165–178. doi:10.1016/j.rse.2013.08.026.

Bury, J.T., Mark, B.G., McKenzie, J.M., et al. (2011) Glacier recession and human vulnerability in the Yanamarey watershed of the Cordillera Blanca, Peru. *Climatic Change*, 105 (1–2): 179–206. doi:10.1007/s10584-010-9870-1.

Cai, J. (2018) *humidity: Calculate Water Vapor Measures from Temperature and Dew Point*. Available at: https://CRAN.R-project.org/package=humidity (Downloaded: 11 May 2019).

Carey, M., Baraer, M., Mark, B.G., et al. (2014) Toward hydro-social modeling: Merging human variables and the social sciences with climate-glacier runoff models (Santa River, Peru). *Journal of Hydrology*, 518: 60–70. doi:10.1016/j.jhydrol.2013.11.006.

Chander, G., Markham, B.L. and Helder, D.L. (2009) Summary of current radiometric calibration coefficients for Landsat MSS, TM, ETM+, and EO-1 ALI sensors. *Remote Sensing of Environment*, 113 (5): 11. doi:10.1016/j.rse.2009.01.007.

Chevallier, P., Pouyaud, B., Suarez, W., et al. (2011) Climate change threats to environment in the tropical Andes: glaciers and water resources. *Regional Environmental Change*, 11 (1): 179–187. doi:10.1007/s10113-010-0177-6.

Condom, T., Escobar, M., Purkey, D., et al. (2012) Simulating the implications of glaciers' retreat for water management: a case study in the Rio Santa basin, Peru. *Water International*, 37 (4): 442–459. doi:10.1080/02508060.2012.706773.

Crumley, R. (2015) *Investigating Glacier Melt Contribution to Stream Discharge and Experiences of Climate Change in the Shullcas River Watershed in Peru*. Masters Thesis, The Ohio State University.

Dewpoint (n.d.). Available at: https://cals.arizona.edu/azmet/dewpoint.html (Accessed: 10 May 2019).

Drenkhan, F., Guardamino, L., Huggel, C., et al. (2018) Current and future glacier and lake assessment in the deglaciating Vilcanota-Urubamba basin, Peruvian Andes. *Global and Planetary Change*, 169: 105–118. doi:10.1016/j.gloplacha.2018.07.005.

Dussaillant, I., Berthier, E., Brun, F., et al. (2019) Two decades of glacier mass loss along the Andes. *Nature Geoscience*, 12 (10): 802–808. doi:10.1038/s41561-019-0432-5.

Dyurgerov, M.B. and Meier, M.F. (2005) *G Glaciers and the changing Earth system: a 2004 snapshot*. *Occas. Pap. 58* 117 pp.,. Institute of Arctic and Alpine Research, University of Colorado Boulder

Farías-Barahona, D., Vivero, S., Casassa, G., et al. (2019) Geodetic Mass Balances and Area Changes of Echaurren Norte Glacier (Central Andes, Chile) between 1955 and 2015. *Remote Sensing*, 11 (3): 260. doi:10.3390/rs11030260.

Favier, V., Wagnon, P., Chazarin, J.-P., et al. (2004) One-year measurements of surface heat budget on the ablation zone of Antizana Glacier 15, Ecuadorian Andes. *Journal of Geophysical Research: Atmospheres*, 109 (D18). doi:10.1029/2003JD004359.

Francou, B., Ribstein, P., Wagnon, P., et al. (2005) "Glaciers of the Tropical Andes: Indicators of Global Climate Variability." In Huber, U.M., Bugmann, H.K.M. and Reasoner, M.A. (eds.) *Global Change and Mountain Regions*. Dordrecht: Springer Netherlands. pp. 197–204. doi:10.1007/1-4020-3508-X_20.

Francou, B. and Vincent, C. (2017) *Les glaciers à l'épreuve du climat*. Référence. Marseille: IRD Éditions. Available at: http://books.openedition.org/irdeditions/9972 (Downloaded: 7 May 2019).

Frey, H. and Paul, F. (2012) On the suitability of the SRTM DEM and ASTER GDEM for the compilation of topographic parameters in glacier inventories. *International Journal of Applied Earth Observation and Geoinformation*, 18: 480–490. doi:10.1016/j.jag.2011.09.020.

Glas, R., Lautz, L., McKenzie, J., et al. (2018) A review of the current state of knowledge of proglacial hydrogeology in the Cordillera Blanca, Peru. *Wiley Interdisciplinary Reviews: Water*, 5 (5): e1299. doi:10.1002/wat2.1299.

Gurgiser, W., Mölg, T., Nicholson, L., et al. (2013) Mass-balance model parameter transferability on a tropical glacier. *Journal of Glaciology*, 59 (217): 845–858. doi:10.3189/2013JoG12J226.

Hanshaw, M.N. and Bookhagen, B. (2014) Glacial areas, lake areas, and snow lines from 1975 to 2012: status of the Cordillera Vilcanota, including the Quelccaya Ice Cap, northern central Andes, Peru. *The Cryosphere*, 8 (2): 359–376. doi:https://doi.org/10.5194/tc-8-359-2014.

Hastenrath, S. (1994) Recession of Tropical Glaciers. *Science*, 265 (5180): 1790–1791. doi:10.1126/science.265.5180.1790.

Heydari, M. and Khalifeloo, M.H. (2015) *Application of different statistical methods to recover missing rainfall data in the Klang River Catchment*. Available at: https://www.academia.edu/14501889/Application_of_different_statistical_methods_to_recover_missing_rainfall_data_in_the_Klang_River_Catchment (Accessed: 10 May 2019).

Hoffman, M.J., Fountain, A.G. and Achuff, J.M. (2007) 20th-century variations in area of cirque glaciers and glacierets, Rocky Mountain National Park, Rocky Mountains, Colorado, USA. *Annals of Glaciology*, 46: 349–354. doi:10.3189/172756407782871233.

Huh, K.I., Mark, B.G., Ahn, Y., et al. (2017) Volume change of tropical Peruvian glaciers from multi-temporal digital elevation models and volume–surface area scaling. *Geografiska Annaler: Series A, Physical Geography*, 99 (3): 222–239. doi:10.1080/04353676.2017.1313095.

Huss, M. (2013) Density assumptions for converting geodetic glacier volume change to mass change. *The Cryosphere*, 7 (3): 877–887. doi:10.5194/tc-7-877-2013.

Kaser, G. and Georges, C. (1997) Changes of the equilibrium-line altitude in the tropical Cordillera Blanca, Peru, 1930–50, and their spatial variations. *Annals of Glaciology*, 24: 344–349. doi:10.3189/S0260305500012428.

Kaser, G. and Georges, C. (1999) On the Mass Balance of Low Latitude Glaciers with Particular Consideration of the Peruvian Cordillera Blanca. *Geografiska Annaler. Series A, Physical Geography*, 81 (4): 643–651.

Kaser, G., Juen, I., Georges, C., et al. (2003) The impact of glaciers on the runoff and the reconstruction of mass balance history from hydrological data in the tropical Cordillera Blanca, Perú. *Journal of Hydrology*, 282 (1–4): 130–144. doi:10.1016/S0022-1694(03)00259-2.

Lemke, P., Ren, J., Alley, R.B., et al. (2007) *Observations: Changes in Snow, Ice and Frozen Ground*. Available at: http://www.cambridge.org/asia/catalogue/catalogue.asp?isbn=9780521880091 (Accessed: 5 May 2019).

Lipton, J.K. (2014) Lasting Legacies: Conservation and Communities at Huascaran National Park, Peru. *Society & Natural Resources*, 27 (8): 820–833. doi:10.1080/08941920.2014.905888.

López-Moreno, J.I., Fontaneda, S., Bazo, J., et al. (2014) Recent glacier retreat and climate trends in Cordillera Huaytapallana, Peru. *Global and Planetary Change*, 112: 1–11. doi:10.1016/j.gloplacha.2013.10.010.

Lynch, B.D. (2012) Vulnerabilities, competition and rights in a context of climate change toward equitable water governance in Peru's Rio Santa Valley. *Global Environmental Change*, 22 (2): 364–373. doi:10.1016/j.gloenvcha.2012.02.002.

Mackay, J.M., Barrand, N.E., Hannah, D.M., Krause, S., Jackson, C.R., Everest, J., MacDonald, A., O Dochartaigh, B. (2020) Proglacial groundwater storage dynamics under climate change and glacier retreat. *Hydrological Processes*, doi:10.1002/hyp.13961

Malz, P., Meier, W., Casassa, G., et al. (2018) Elevation and Mass Changes of the Southern Patagonia Icefield Derived from TanDEM-X and SRTM Data. *Remote Sensing*, 10 (2): 188. doi:10.3390/rs10020188.

Mark, B.G., Bury, J., McKenzie, J.M., et al. (2010) Climate Change and Tropical Andean Glacier Recession: Evaluating Hydrologic Changes and Livelihood Vulnerability in the Cordillera Blanca, Peru. *Annals of the Association of American Geographers*, 100 (4): 794–805. doi:10.1080/00045608.2010.497369.

Mark, B.G., French, A., Baraer, M., et al. (2017) Glacier loss and hydro-social risks in the Peruvian Andes. *Global and Planetary Change*, 159: 61–76. doi:10.1016/j.gloplacha.2017.10.003.

Mark, B.G. and Seltzer, G.O. (2005) Evaluation of recent glacier recession in the Cordillera Blanca, Peru (AD 1962–1999): spatial distribution of mass loss and climatic forcing. *Quaternary Science Reviews*, 24 (20–21): 2265–2280. doi:10.1016/j.quascirev.2005.01.003.

Military Specification [MIL]-T-89101(DMA). (1981) Tactical Pilotage Charts (TPC), *Defence Mapping Agency*

Milner, A.M., K. Khamis, T.J. Battin, J.E. Brittain, N.E. Barrand, L. Fuereder, S. Cauvy-Fraunie, G.M. Gislason, D. Jacobsen, D.M. Hannah, A.J. Hodson, E. Hood, V. Lencioni, J.S. Olafsson, C.T. Robinson, M. Tranter & L.E. Brown (2017) 'Glacier shrinkage driving global changes in downstream systems.' *Proceedings of the National Academy of Sciences*, 114 (37), 9770-9776, doi:10.1073/pnas.1619807114.

Pfeffer, W. T., Arendt, A. A., Bliss, A., Bolch, T., Cogley, J. G.,Gardner, A. S., Hagen, J. O., Hock, R., Kaser, G., Kienholz,C., Miles, E. S., Moholdt, G., Molg, N., Paul, F., Radic, V.,Rastner, P., Raup, B. H., Rich, J., Sharp, M. J., Andeassen, L.M., Bajracharya, S., Barrand, N. E., Beedle, M. J., Berthier, E.,Bhambri, R., Brown, I., Burgess, D. O., Burgess, E. W., Cawkwell, F., Chinn, T., Copland, L., Cullen, N. J., Davies, B., DeAngelis, H., Fountain, A. G., Frey, H., Giffen, B. A., Glasser,N. F., Gurney, S. D., Hagg, W., Hall, D. K., Haritashya, U. K.,Hartmann, G., Herreid, S., Howat, I., Jiskoot, H., Khromova, T.E., Klein, A., Kohler, J., Konig, M., Kriegel, D., Kutuzov, S.,Lavrentiev, I., Le Bris, R., Li, X., Manley, W. F., Mayer, C.,Menounos, B., Mercer, A., Mool, P., Negrete, A., Nosenko, G.,Nuth, C., Osmonov, A., Pettersson, R., Racoviteanu, A., Ranzi,R., Sarikaya, M. A., Schneider, C., Sigurdsson, O., Sirguey, P.,Stokes, C. R., Wheate, R., Wolken, G. J., Wu, L. Z., Wyatt,F. R., and Consortium, R.: The Randolph Glacier Inventory: a globally complete inventory of glaciers, J. Glaciol., 60, 537–552,doi:10.3189/2014jog13j176, 2014.

Polk, M.H., Young, K.R., Baraer, M., et al. (2017) Exploring hydrologic connections between tropical mountain wetlands and glacier recession in Peru's Cordillera Blanca. *Applied Geography*, 78: 94–103. doi:10.1016/j.apgeog.2016.11.004.

Rabatel, A., Francou, B., Soruco, A., et al. (2013) Current state of glaciers in the tropical Andes: a multi-century perspective on glacier evolution and climate change. *The Cryosphere*, 7 (1): 81–102. doi:10.5194/tc-7-81-2013.

Racoviteanu, A.E., Arnaud, Y., Williams, M.W., et al. (2008) Decadal changes in glacier parameters in the Cordillera Blanca, Peru, derived from remote sensing. *Journal of Glaciology*, 54 (186): 499–510.

Ramos-Calzado, P., Gómez-Camacho, J., Pérez-Bernal, F., et al. (2008) A novel approach to precipitation series completion in climatological datasets: application to Andalusia. *International Journal of Climatology*, 28 (11): 1525–1534. doi:10.1002/joc.1657.

Rasmussen, M.B. (2017) Water Futures: Contention in the Construction of Productive Infrastructure in the Peruvian Highlands. *Anthropologica*. doi:10.3138/anth.582.T04.

Schauwecker, S., Rohrer, M., Acuña, D., et al. (2014) Climate trends and glacier retreat in the Cordillera Blanca, Peru, revisited. *Global and Planetary Change*, 119: 85–97. doi:10.1016/j.gloplacha.2014.05.005.

Schauwecker, S., Rohrer, M., Huggel, C., et al. (2017) The freezing level in the tropical Andes, Peru: An indicator for present and future glacier extents. *Journal of Geophysical Research: Atmospheres*, 122 (10): 5172–5189. doi:10.1002/2016JD025943.

Seehaus, T., Malz, P., Sommer, C., et al. (2019) Changes of the tropical glaciers throughout Peru between 2000 and 2016 - Mass balance and area fluctuations. *The Cryosphere Discussions*, pp. 1–34. doi:10.5194/tc-2018-289.

Silverio, W. and Jaquet, J.-M. (2017) Evaluating glacier fluctuations in Cordillera Blanca (Peru) by remote sensing between 1987 & 2016 in the context of ENSO. *Archives des Sciences*, 69: 145–161.

USGS (2018) *Landsat 7 (L7) Data Users Handbook*.

USGS (2019) *LANDSAT 8 (L8) DATA USERS HANDBOOK*. Available at: https://prd-wret.s3-us-west-2.amazonaws.com/assets/palladium/production/atoms/files/LSDS-1574_L8_Data_Users_Handbook_v4.0.pdf (Accessed: 10 May 2019).

Vaisala Oyj (2013) *HUMIDITY CONVERSION FORMULAS: Calculation formulas for humidity*. Helsinki, Finland: Vaisala.

Veettil, B.K. (2018) Glacier mapping in the Cordillera Blanca, Peru, tropical Andes, using Sentinel-2 and Landsat data. *Singapore Journal of Tropical Geography*, 39 (3): 351–363. doi:10.1111/sjtg.12247.

Veettil, B.K., Wang, S., Florêncio de Souza, S., et al. (2017) Glacier monitoring and glacier-climate interactions in the tropical Andes: A review. *Journal of South American Earth Sciences*, 77: 218–246. doi:10.1016/j.jsames.2017.04.009.

Veettil, B.K., Wang, S., Simões, J.C., et al. (2018) Regional climate forcing and topographic influence on glacier shrinkage: eastern cordilleras of Peru. *International Journal of Climatology*, 38 (2): 979–995. doi:10.1002/joc.5226.

Vergara, W., Deeb, A., Valencia, A., et al. (2007) Economic impacts of rapid glacier retreat in the Andes. *Eos, Transactions American Geophysical Union*, 88 (25): 261–264. doi:10.1029/2007EO250001.

Vuille, M. and Bradley, R.S. (2000) Mean annual temperature trends and their vertical structure in the tropical Andes. *Geophysical Research Letters*, 27 (23): 3885–3888. doi:10.1029/2000GL011871.

Vuille, M., Bradley, R.S., Werner, M., et al. (2003) "20th century climate change in the tropical Andes: observations and model results." In *Climate variability and change in high elevation regions: Past, present & future*. Springer. pp. 75–99.

Vuille, M., Carey, M., Huggel, C., et al. (2018) Rapid decline of snow and ice in the tropical Andes – Impacts, uncertainties and challenges ahead. *Earth-Science Reviews*, 176: 195–213. doi:10.1016/j.earscirev.2017.09.019.

Vuille, M., Francou, B., Wagnon, P., et al. (2008a) Climate change and tropical Andean glaciers: Past, present and future. *Earth-Science Reviews*, 89 (3–4): 79–96. doi:10.1016/j.earscirev.2008.04.002.

Vuille, M., Kaser, G. and Juen, I. (2008b) Glacier mass balance variability in the Cordillera Blanca, Peru and its relationship with climate and the large-scale circulation. *Global and Planetary Change*, 62 (1–2): 14–28. doi:10.1016/j.gloplacha.2007.11.003.

Wagnon, P., Ribstein, P., Francou, B., et al. (1999a) Annual cycle of energy balance of Zongo Glacier, Cordillera Real, Bolivia. *Journal of Geophysical Research: Atmospheres*, 104 (D4): 3907–3923. doi:10.1029/1998JD200011.

Wagnon, P., Ribstein, P., Kaser, G., et al. (1999b) Energy balance and runoff seasonality of a Bolivian glacier. *Global and Planetary Change*, 22 (1): 49–58. doi:10.1016/S0921-8181(99)00025-9.

WGI (1989) *World glacier inventory: Status 1988: a contribution to the Global Environment Monitoring System (GEMS) and the International Hydrological Programme*. Haeberli, W., Bosch, H., Scherler, K., et al. (eds.). Wallingford: International Association of Hydrological Sciences [u.a.].

Wigmore, O. and Mark, B. (2017) Monitoring tropical debris-covered glacier dynamics from high-resolution unmanned aerial vehicle photogrammetry, Cordillera Blanca, Peru. *The Cryosphere*, 11 (6): 2463–2480. doi:https://doi.org/10.5194/tc-11-2463-2017.

Zuur, A.F., Ieno, E.N. and Smith, G.M. (2007) *Analysing Ecological Data*. New York, NY, UNITED STATES: Springer. Available at: http://ebookcentral.proquest.com/lib/bham/detail.action?docID=371384 (Downloaded: 11 May 2019).

Figure 1

Location map of study sites in the Cordillera Blanca (see inset map A, including glacier sub-populations A1-A3) and Cordillera Huaytapallana (inset map B). RGI outlines of glaciers are shown in blue (Pfeffer et al., 2014), along with major river systems, river catchments, and SENAHMI meteorological stations. Background elevation colour scale is from NASA Shuttle Radar Topography Mission (SRTM) 1 arc-second data.

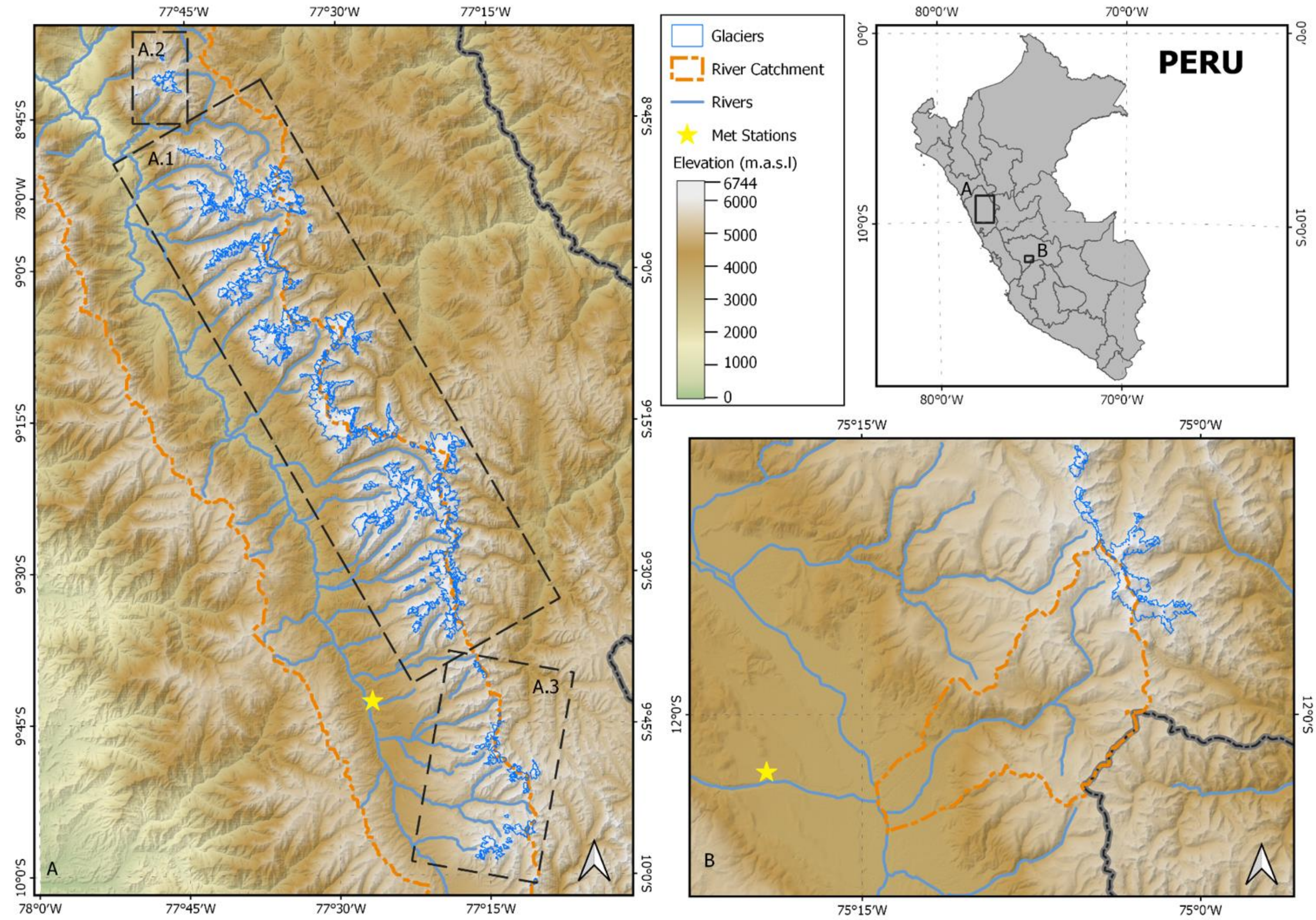

Figure 2 – Maps of annual glacier ice surface elevation change (m yr^{-1}) from 1972 t0 2018 at the Cordillera Blanca (A) and Cordillera Huaytapallana (B), Peru. Glacier sub-regional population location maps are shown in Figure 1.

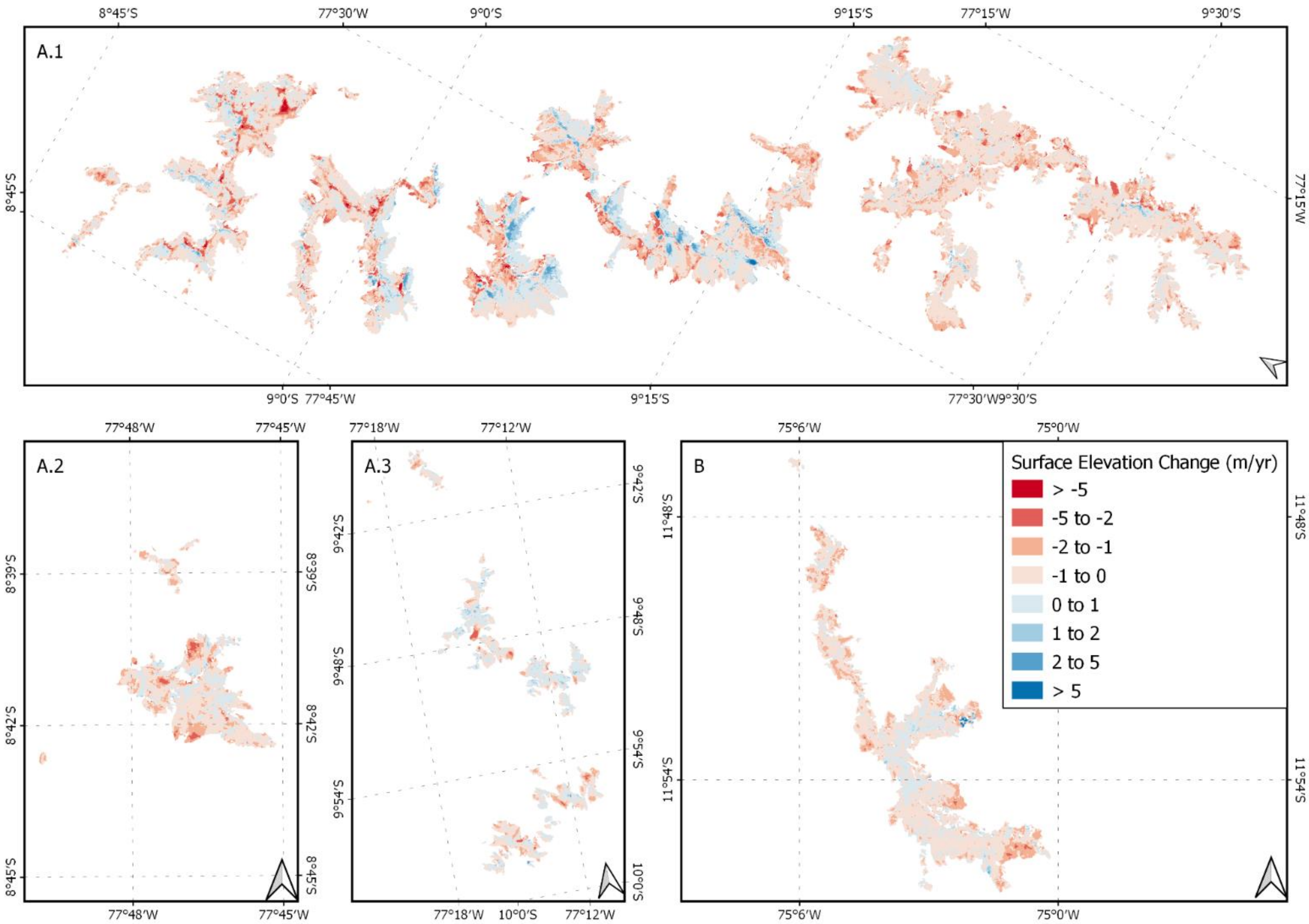

Figure 3 – Annual surface elevation change (m/yr) from 1972 to 2018 for individual glaciers of the Cordillera Blanca (A) and Cordillera Huaytapallana (B). Sub-region locations are shown on Figure 1.

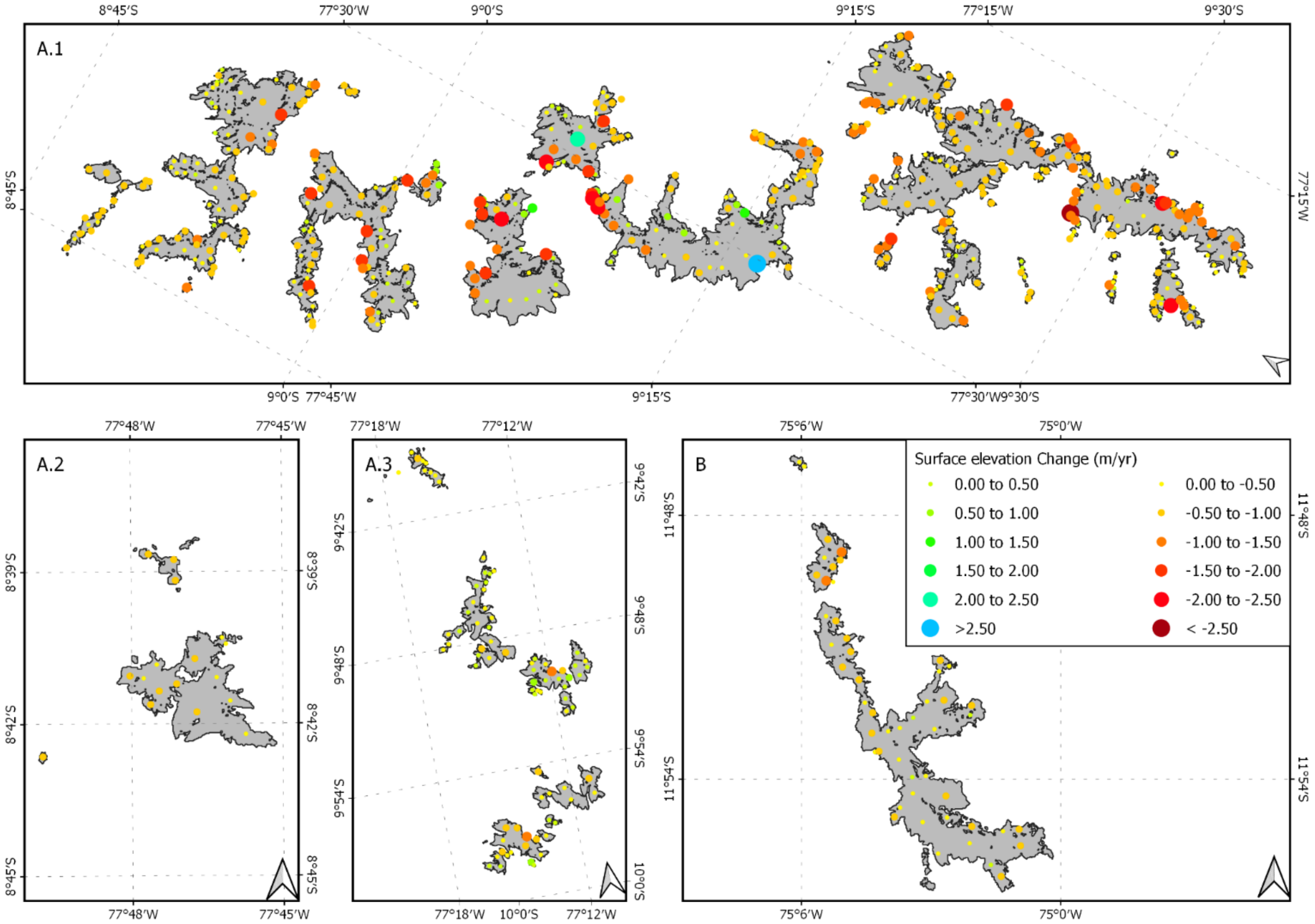

Figure 4 – Glacier hypsometry (filled line) and mass balance (points, myr^{-1} w.e.) from 1972-2018 for the Cordillera Blanca (A) and Cordillera Huaytapallana (B). Ice covered are is calculated for each of the 250m altitudinal bands in order to calculate the Hypsometry.

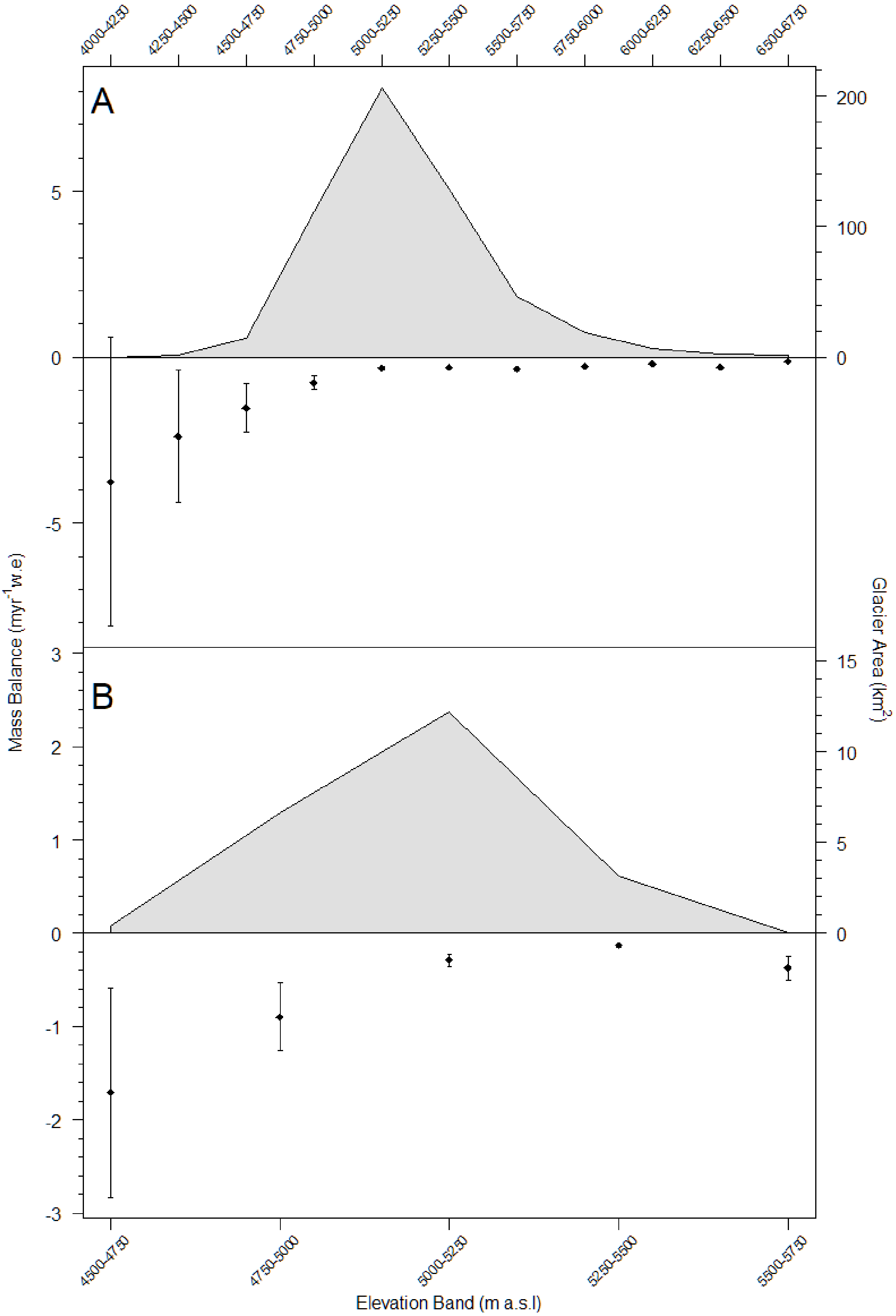

Figure 5 – Annual trends in Cordillera Blanca Temperature (A), Precipitation (C) and Humidity (E) from the Recuay meteorological station; and annual trends in Cordillera Huaytapallana Temperature (B), Precipitation (D) and Humidity (F) from the Huayao meteorological station.

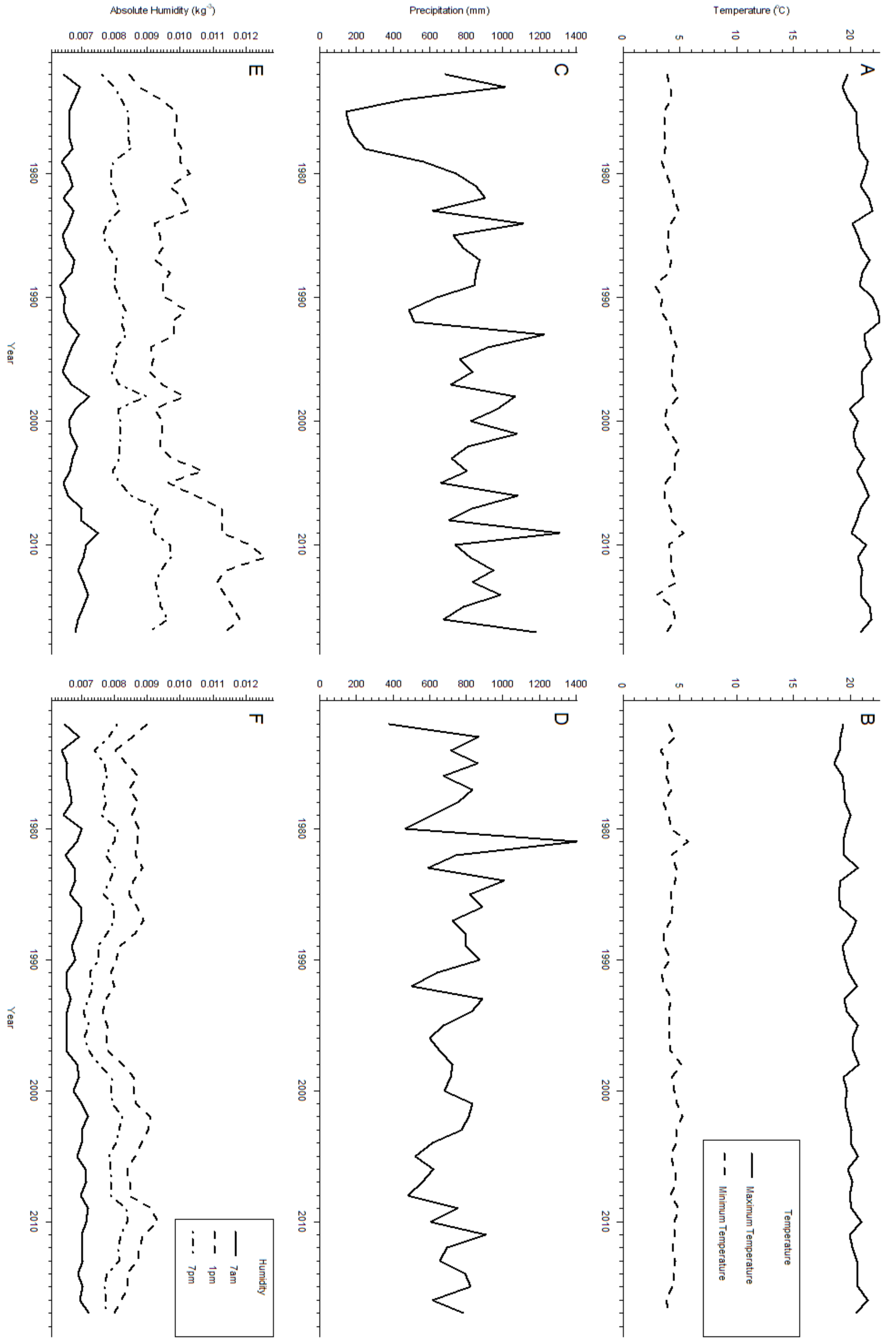

Figure 6 – Cordillera Blanca Mass Balance (dotted lines, m w.e.) and Meteorological Variables (solid lines) from 1972-2017. Five Year Rolling Averages of Meteorological Variables are Presented (red lines) with Linear Trend Lines for Meteorological Variables (blue lines) Across Each of the Three Analysed Mass Balance Periods (1972-1986, 1986-2000, 2000-2017)

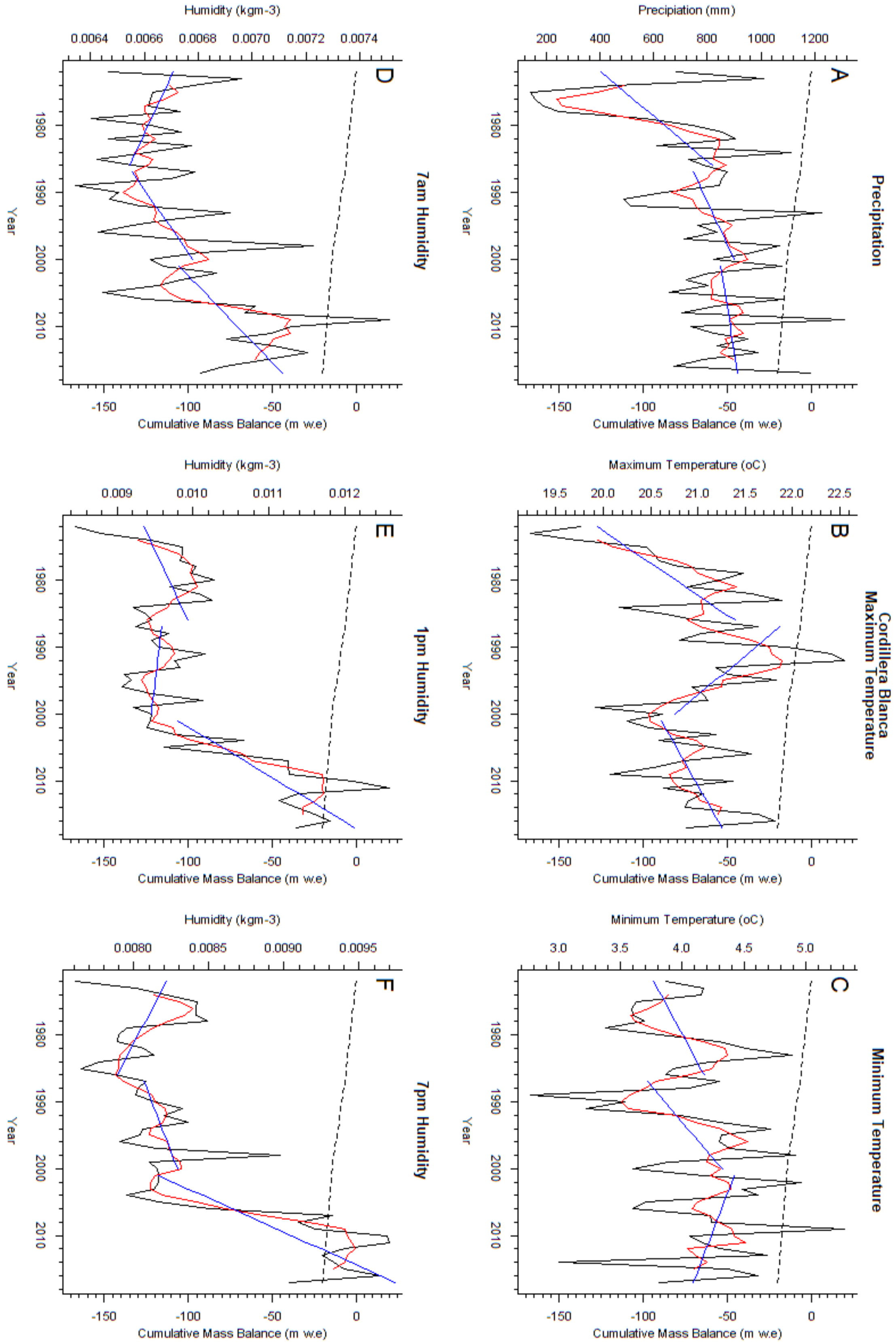

Figure 7 – Cordillera Blanca (5250-5500 m a.s.l) Mass Balance (dotted lines, m w.e.) and Meteorological Variables (solid lines) from 1972-2017. Five Year Rolling Averages of Meteorological Variables are Presented (red lines) with Linear Trend Lines for Meteorological Variables (blue lines) Across Each of the Three Analysed Mass Balance Periods (1972-1986, 1986-2000, 2000-2017)

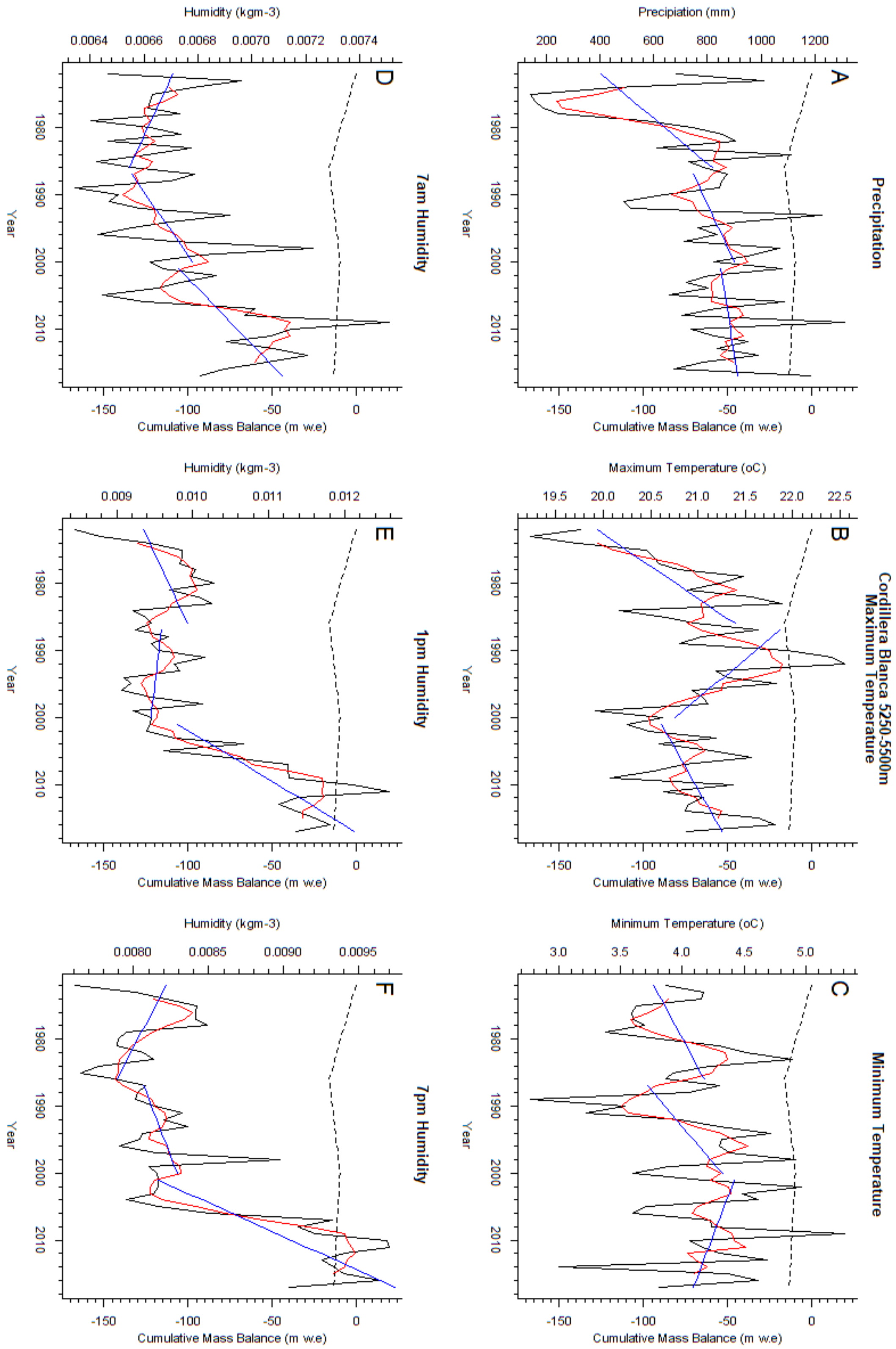

Figure 8 – Cordillera Blanca (5000-5250 m a.s.l) Mass Balance (dotted lines, m w.e.) and Meteorological Variables (solid lines) from 1972-2017. Five Year Rolling Averages of Meteorological Variables are Presented (red lines) with Linear Trend Lines for Meteorological Variables (blue lines) Across Each of the Three Analysed Mass Balance Periods (1972-1986, 1986-2000, 2000-2017)

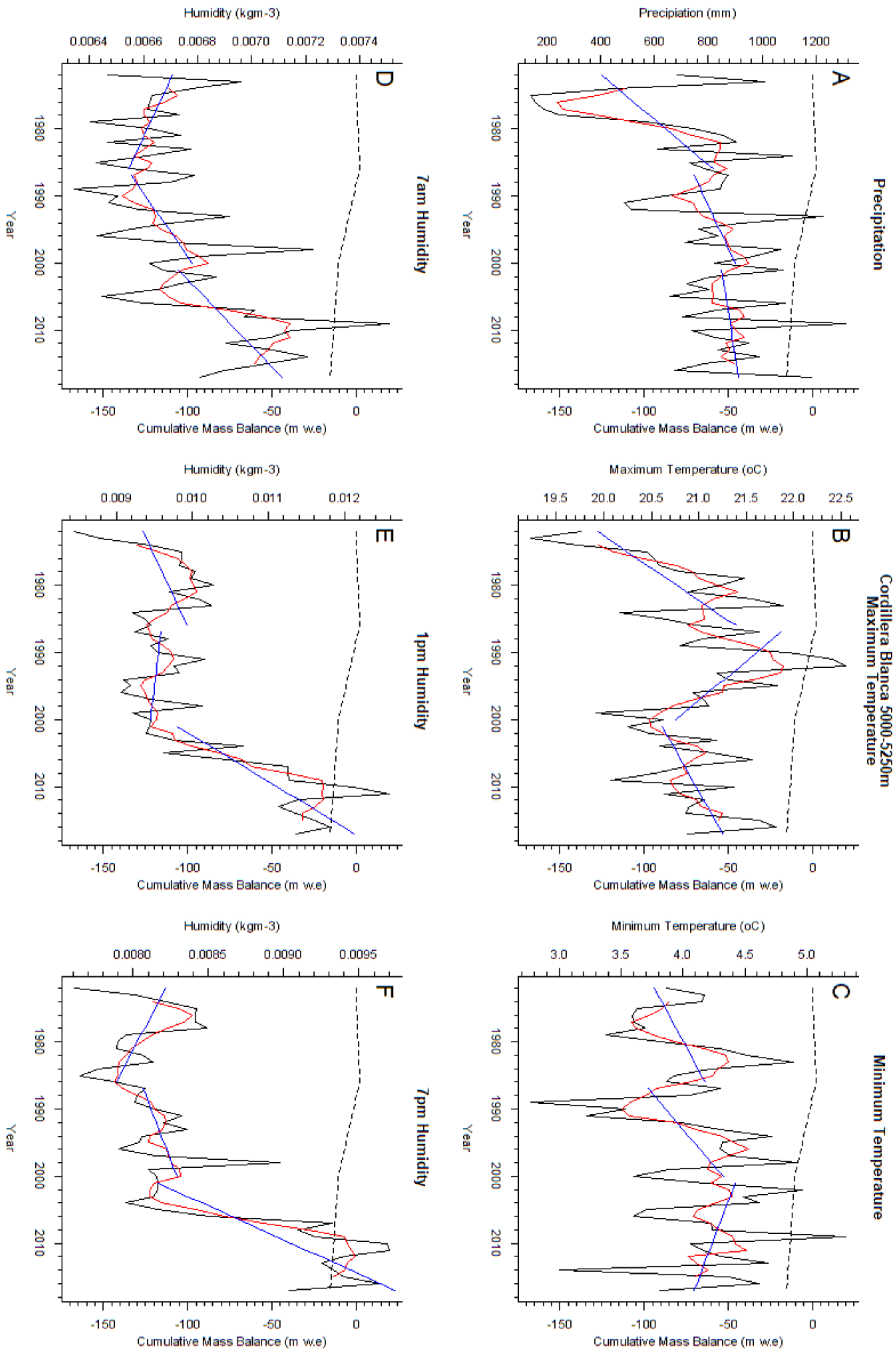

Figure 9 – Cordillera Blanca (North) Mass Balance (dotted lines, m w.e.) and Meteorological Variables (solid lines) from 1972-2017. Five Year Rolling Averages of Meteorological Variables are Presented (red lines) with Linear Trend Lines for Meteorological Variables (blue lines) Across Each of the Three Analysed Mass Balance Periods (1972-1986, 1986-2000, 2000-2017)

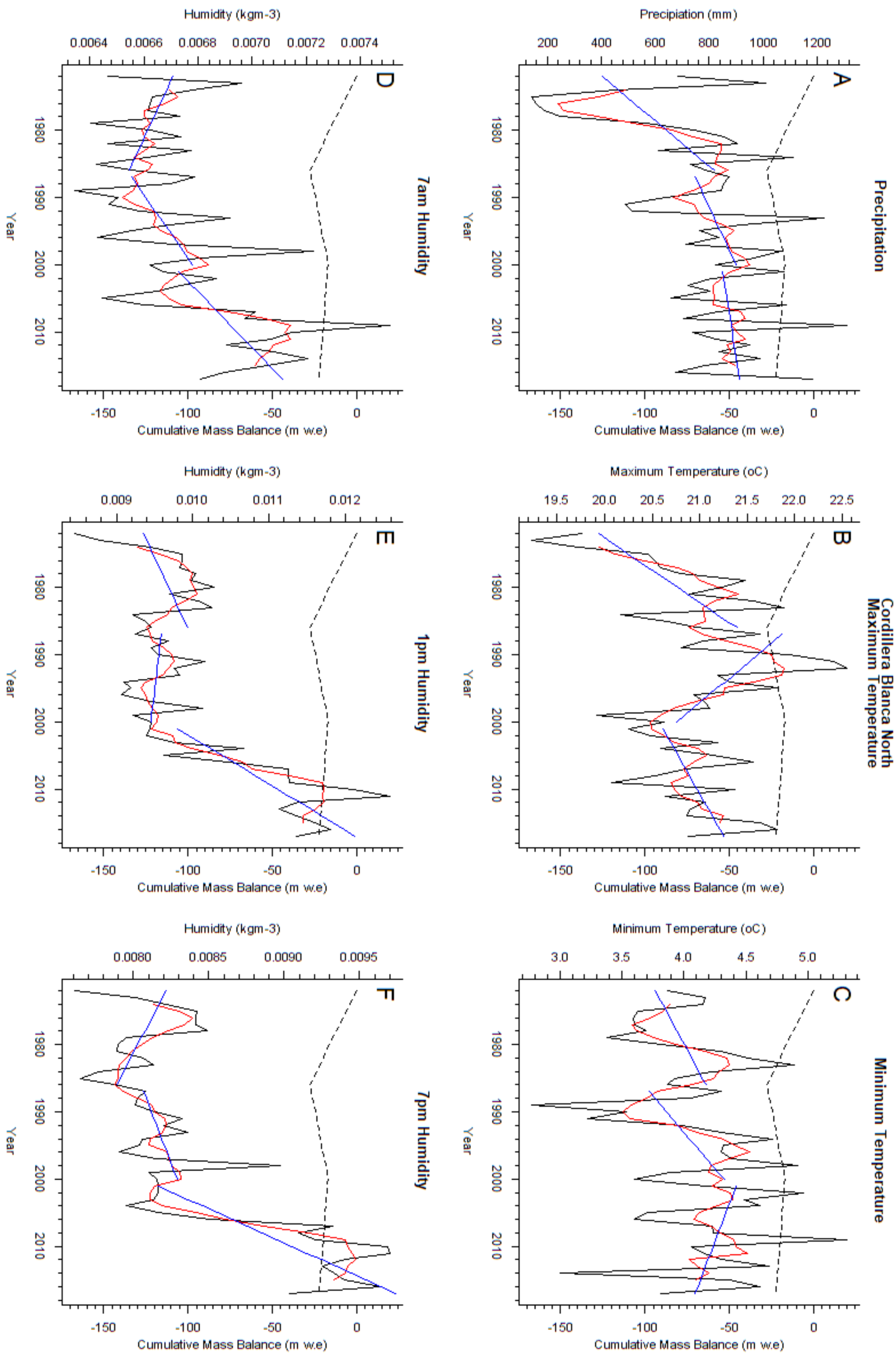

Figure 10 – Cordillera Blanca (South) Mass Balance (dotted lines, m w.e.) and Meteorological Variables (solid lines) from 1972-2017. Five Year Rolling Averages of Meteorological Variables are Presented (red lines) with Linear Trend Lines for Meteorological Variables (blue lines) Across Each of the Three Analysed Mass Balance Periods (1972-1986, 1986-2000, 2000-2017)

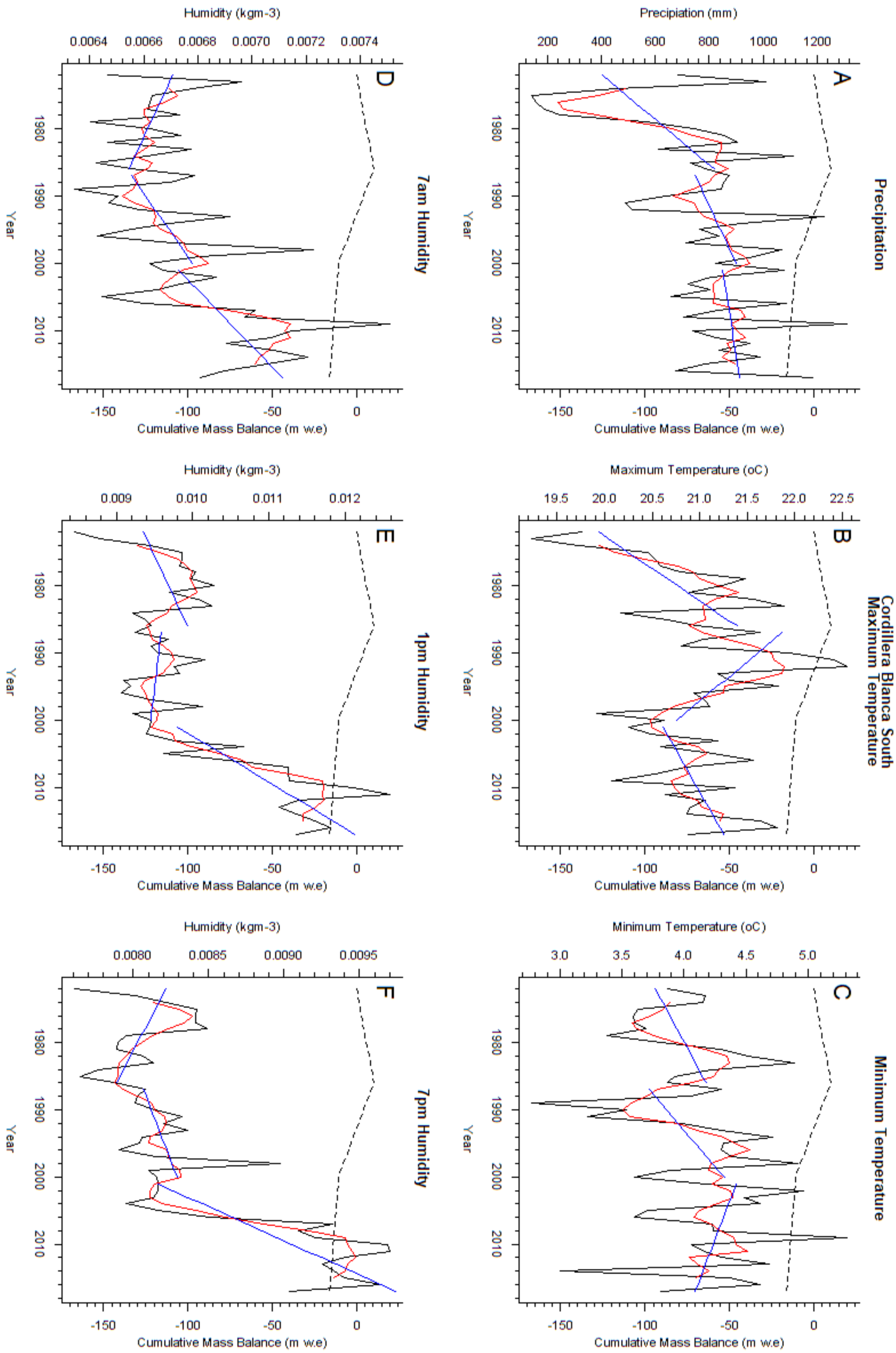

Figure 11 – Cordillera Huaytapallana Mass Balance (dotted lines, m w.e.) and Meteorological Variables (solid lines) from 1972-2017. Five Year Rolling Averages of Meteorological Variables are Presented (red lines) with Linear Trend Lines for Meteorological Variables (blue lines) Across Each of the Three Analysed Mass Balance Periods (1972-1986, 1986-2000, 2000-2017)

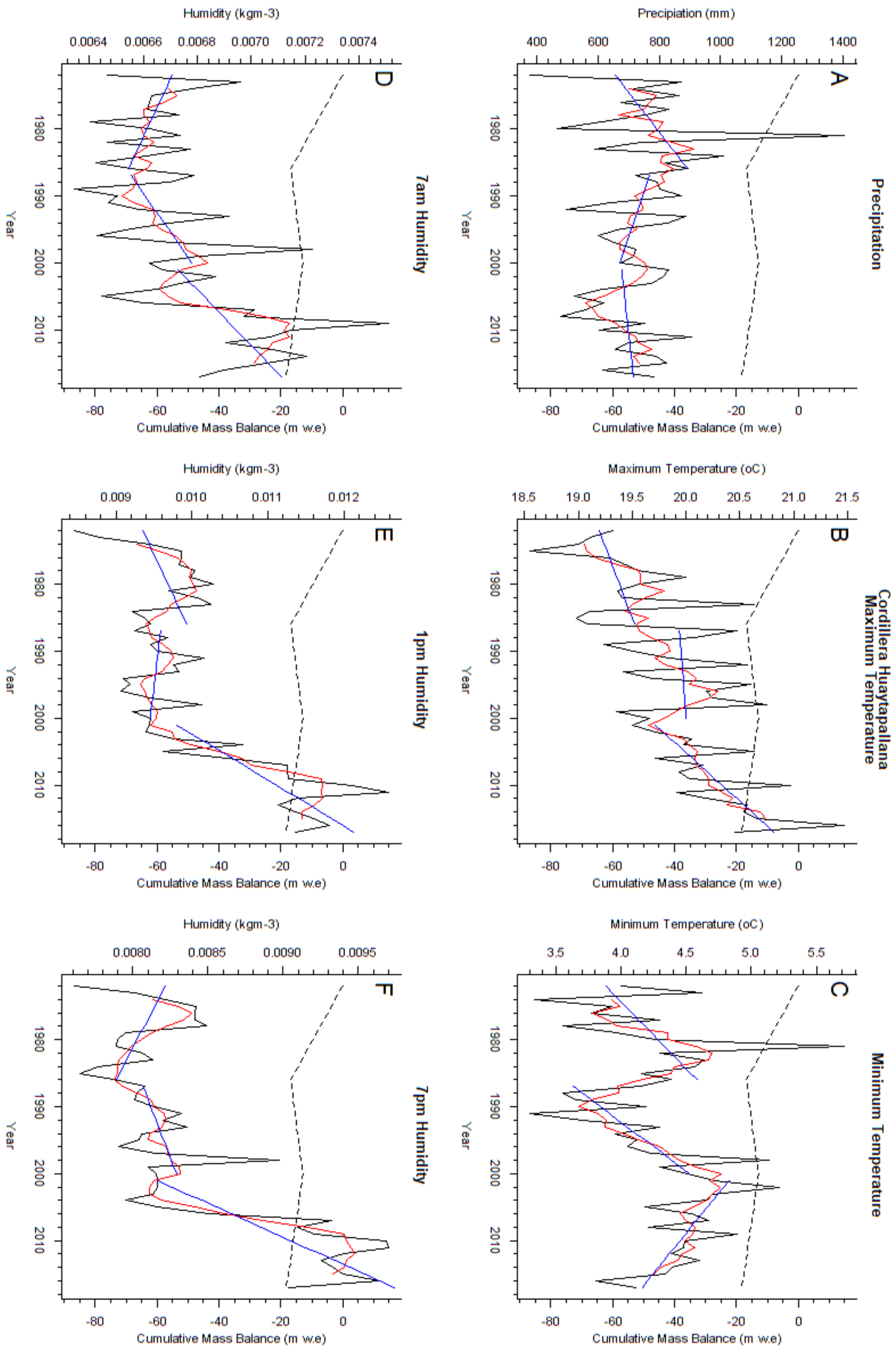

Figure 12 – Cordillera Huaytapallana (4750-5000 m a.s.l)_Mass Balance (dotted lines, m w.e.) and Meteorological Variables (solid lines) from 1972-2017. Five Year Rolling Averages of Meteorological Variables are Presented (red lines) with Linear Trend Lines for Meteorological Variables (blue lines) Across Each of the Three Analysed Mass Balance Periods (1972-1986, 1986-2000, 2000-2017)

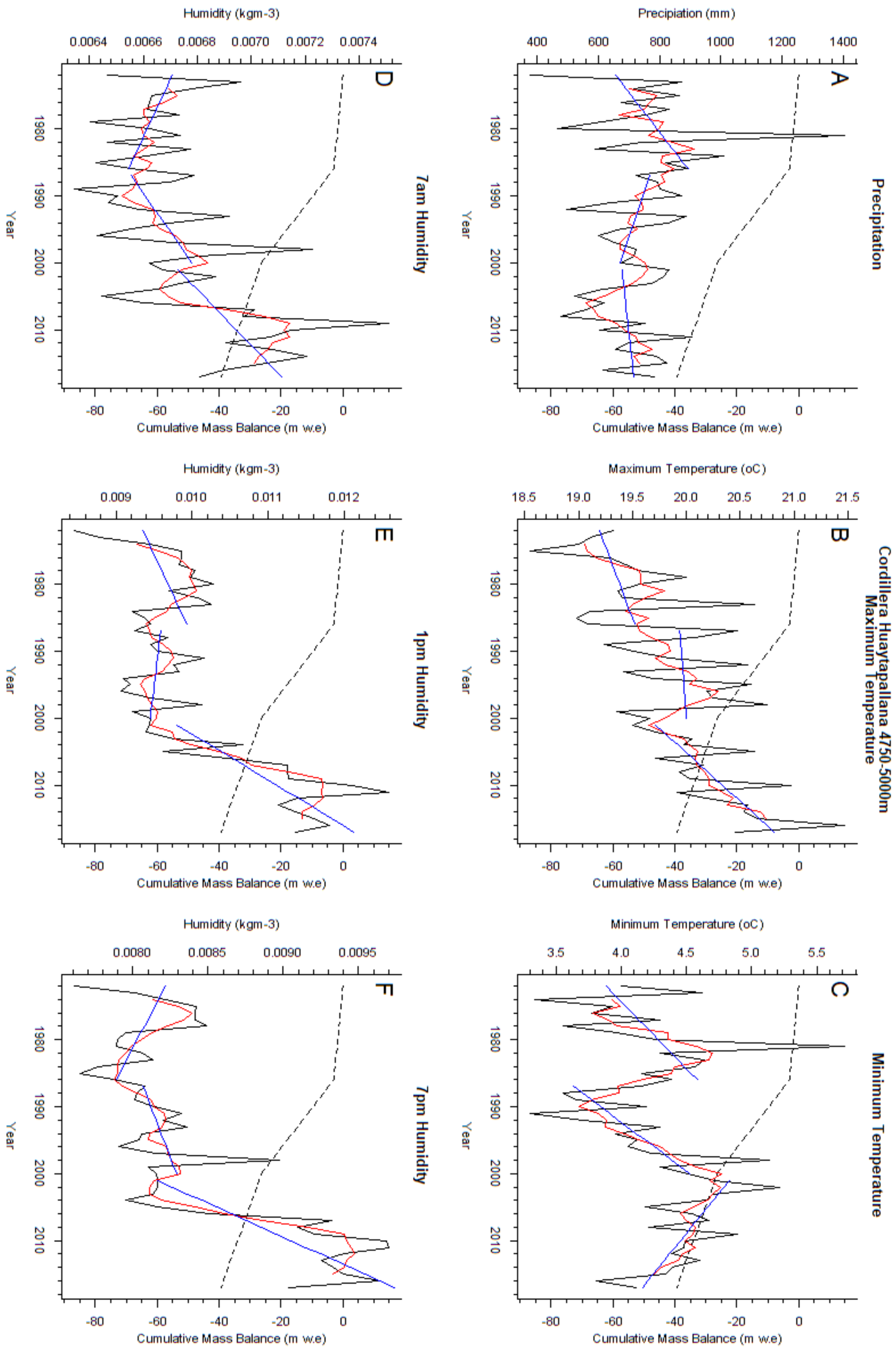

Figure 13 – Cordillera Huaytapallana (5000-5250 m a.s.l)_Mass Balance (dotted lines, m w.e.) and Meteorological Variables (solid lines) from 1972-2017. Five Year Rolling Averages of Meteorological Variables are Presented (red lines) with Linear Trend Lines for Meteorological Variables (blue lines) Across Each of the Three Analysed Mass Balance Periods (1972-1986, 1986-2000, 2000-2017)

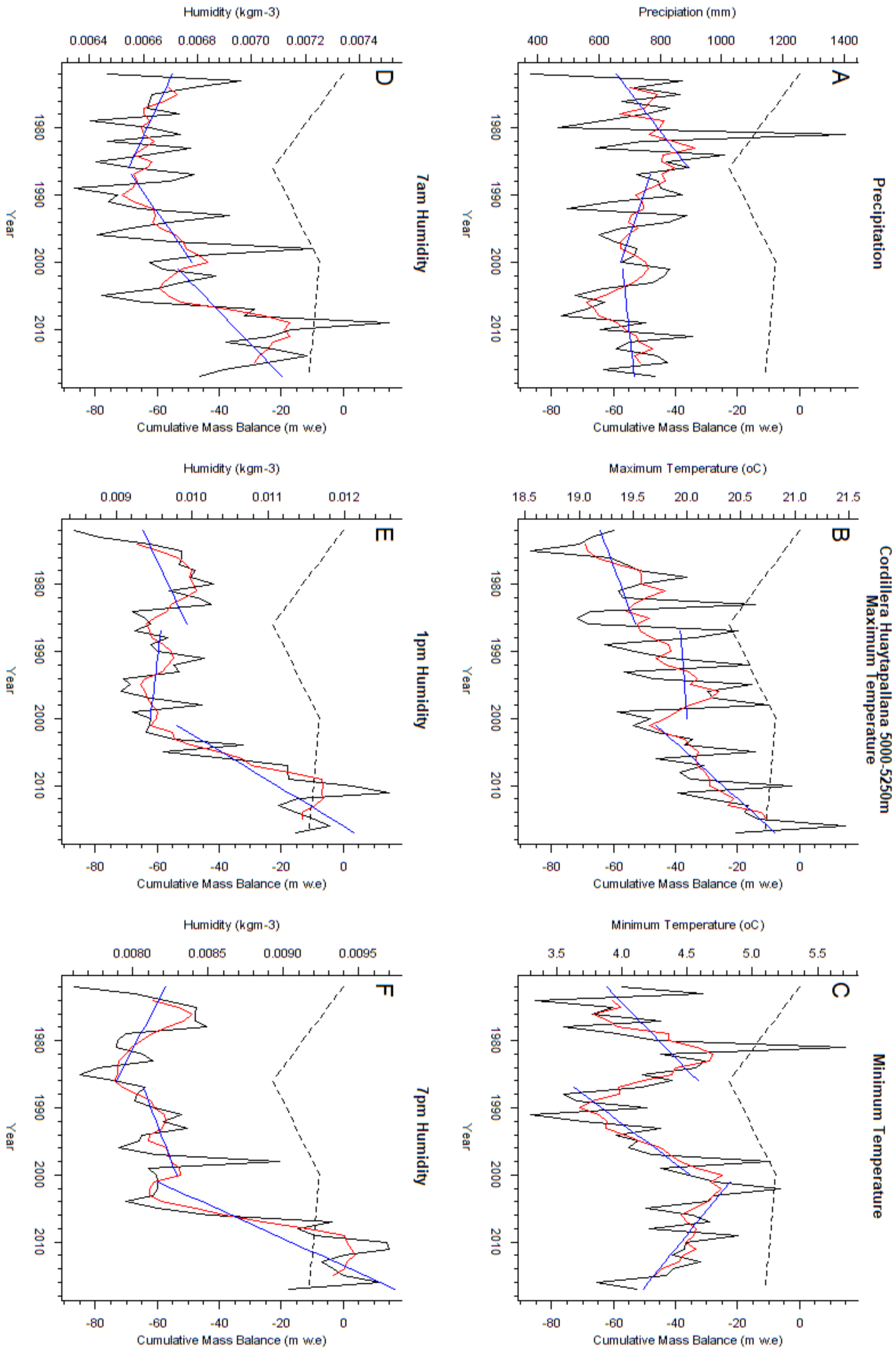

Table 1 – Landsat images used for analysis

Mountain Range	DEM Year	Date	Sensor	Path/Row
Cordillera Blanca	1972/1986	21/08/1988	Landsat 5 - Thematic Mapper	008/066
Cordillera Blanca	1972/1986	21/08/1988	Landsat 5 - Thematic Mapper	008/067
Cordillera Blanca	2000	02/09/1998	Landsat 5 - Thematic Mapper	008/066
Cordillera Blanca	2000	02/09/1998	Landsat 5 - Thematic Mapper	008/067
Cordillera Blanca	2018	09/09/2018	Landsat 8 - Operational Land Imager	008/066
Cordillera Blanca	2018	09/09/2018	Landsat 8 - Operational Land Imager	008/067
Cordillera Huaytapallana	1972/1986	15/08/1985	Landsat 5 - Thematic Mapper	006/068
Cordillera Huaytapallana	2000	06/08/1999	Landsat 5 - Thematic Mapper	006/068
Cordillera Huaytapallana	2018	07/08/2017	Landsat 8 - Operational Land Imager	006/068

Table 2 - Results of multiple linear regression between cumulative mass balance and annual meteorological series

Mountain Range	Predictive Parameters	Coefficient	β Coefficient	p	Intercept	R^2	p (overall)
Blanca	1pm AH	3063.0	0.235	0.058	-0.775	0.417	<0.001
	7am AH	4955.0	0.400	0.002			
	Precipitation	-0.012	-0.509	0.001			
	Max. Temperature	-2.861	-0.312	0.010			
Huaytapallana	Precipitation	-0.009	-0.316	0.018	93.619	0.373	<0.001
	Max. Temperature	-5.047	-0.687	<0.001			